Structural analysis of the Western Afar Margin, East Africa: evidence for multiphase rotational rifting

F. Zwaan[1]†, G. Corti[2], F.Sani[1], D. Keir[1,3], A. Muluneh[4], F. Illsley-Kemp[5], M. Papini[1]

[1] Dipartimento di Scienze della Terra, Università degli Studi di Firenze, Via G. La Pira, 4, 50121 Florence, Italy

[2] Consiglio Nazionale delle Ricerche, Istituto di Geoscienze e Georisorse, Via G. La Pira, 4, 50121 Florence, Italy

[3] School of Ocean and Earth Science, University of Southampton, Southampton SO14 3ZH, UK

[4] School of Earth Sciences, Addis Ababa University, P.O. Box 1176, Addis Abeba, Ethiopia

[5] School of Geography, Environment and Earth Sciences, Victoria University of Wellington, PO Box 600, Wellington 6140, New Zealand

†current address: Institut für Geologie, Universität Bern, Baltzerstrasse 1+3, CH3012 Bern, Switzerland

Corresponding author: Frank Zwaan (frank.zwaan@geo.unibe.ch)

Key Points:

- Structural, borehole and seismicity data from the Western Afar Margin serve to study continental break-up processes and rotational rifting
- Antithetic faults bounding marginal grabens are currently accommodating significant deformation along the margin
- Current extension is due to rotation of the Danakil Block; a previous oblique extension phase was likely related to Arabian plate motion

An edited version of this paper was published by AGU. Copyright (2020) American Geophysical Union

https://doi.org/10.1029/2019TC006043

Zwaan, F., Corti, G., Sani, F., Keir, D., Muluneh, A. A., Illsley-Kemp, F., & Papini, M. (2020). Structural analysis of the Western Afar Margin, East Africa: Evidence for multiphase rotational rifting. Tectonics, 39, e2019TC006043

Abstract

The Afar region in East Africa represents a key location to study continental break-up. We present an integrated structural analysis of the Western Afar Margin (WAM) aiming to better understand rifted margin development and the role of plate rotation during rifting. New structural information from remote sensing, fieldwork and earthquake datasets reveals that the N-S striking WAM is still actively deforming, and is characterized by NNW-SSE normal faulting and a series of marginal grabens. Seismicity distribution analysis and the first-ever borehole-calibrated sections of this developing passive margin show recent slip concentrated along antithetic faults.

Tectonic stress parameters derived from earthquake focal mechanisms reveal different extension directions along the WAM (82˚N), in Afar (66˚N) and in the Main Ethiopian Rift (108˚N). Fault slip analysis along the WAM yields the same extension direction. Combined with GPS data this shows that current tectonics in Afar is dominated by the local rotation of the Danakil Block, considered to have occurred since 11 Ma. Earlier stages of Afar development (since 31-25 Ma) were most likely related to the large-scale rotation of the Arabian plate.

Various authors have proposed scenarios for the evolution of the WAM. Any complete model should consider, among other factors, the multi-phase tectonic history and antithetic fault activity of the margin. The findings of this study are not only relevant for a better understanding of the WAM, but also provide insights into the role of multiphase rotational extension during rifting and passive margin formation in general.

Plain Language Summary

The Earth's continents are in gradual but perpetual motion, driven by large plate tectonic forces in the Earth's deep interior. A crucial process is the stretching and breaking up of continents, initially forming localized rift or graben depressions, followed by the opening of a new ocean flanked by the margins of the newly divided continents (passive margins). Rifts and passive margins are important because of their vast resource potential (e.g. oil, gas, geothermal energy), but pose also severe risks (volcanism, earthquakes and landslides) since they are often home to large populations.

We focus on the Western Afar Margin in Ethiopia, where the African continent is currently splitting apart, providing a unique research opportunity. In the framework of an international collaborative effort, we combined satellite imagery, topography data, field observations, GPS and earthquake measurements in order to map out the present-day geology and tectonic activity along the margin.

Our results show the complexity of tectonic plate movements: we find evidence for two phases of continental stretching in Ethiopia, that both involve the rotation of tectonic plates. We also observe active faulting, which may help to assess seismic risks in the area. Our study helps to better understand passive margins worldwide.

1. Introduction

1.1. Rifting and rotational extension

Extension of the lithosphere, leading to rifting and break-up of continents is an integral part of the global plate tectonic system and a thorough understanding of the processes involved is of great interest for scientific, economic and societal reasons. Rifts and passive margins hold extensive sedimentary archives containing crucial information regarding global change, as well as vast resource potential (e.g. oil, gas, geothermal energy), but pose also severe risks in the shape of volcanism, earthquakes and (submarine) landslides, especially since these areas of the world are often home to large populations (e.g. Haq et al. 1987; Catuneanu et al. 2009; Kirschner et al. 2010; Levell et al. 2011; Davison & Underhill 2012; Zou et al. 2015; Brune 2016). However, a common challenge to researchers is that once breakup occurs and passive margins are formed, the remnants of the once active continental rift is often situated offshore and mostly covered by thick (post-rift) sedimentary sequences (e.g. Argent et al. 2000; Straume et al. 2019). Hence the Afar region in East Africa represents a unique opportunity to study extensional processes and associated structures (e.g. fault geometries and kinematics); it contains active rifts in various stages of maturity, from initial continental rifting to continental break-up, oceanic spreading and passive margin formation, all accessible onshore (e.g. Varet 2018; Illsley-Kemp et al. 2018b; Fig. 1).

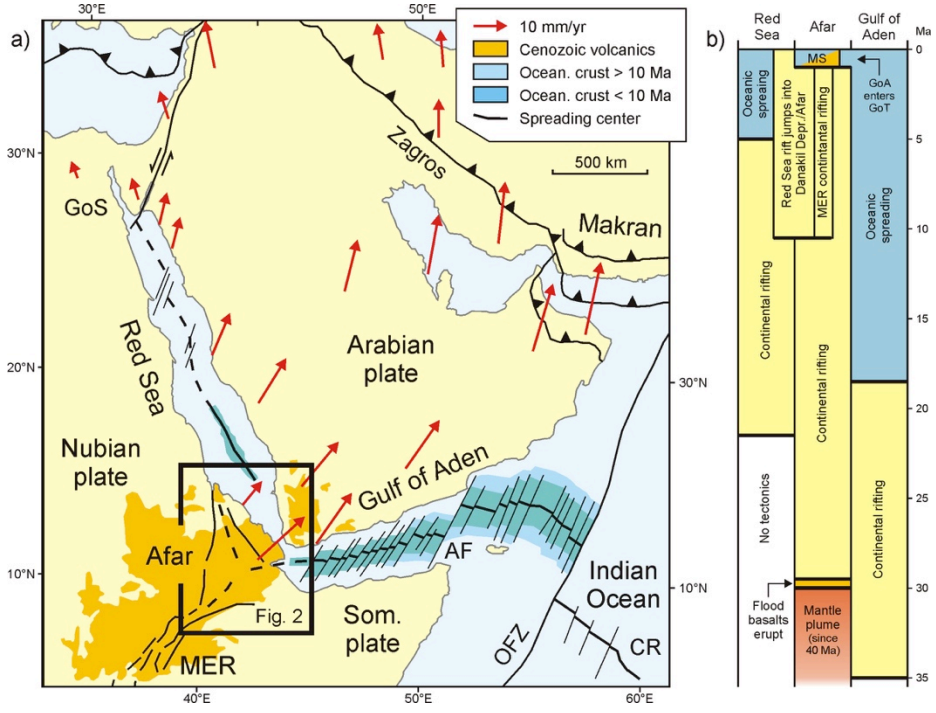

Fig. 1. (a) Tectonic setting of Red Sea-Afar-Gulf of Aden rift system (Modified after Bosworth 2015). Note the westward decreasing width of the oceanic crust as a result of the rotation of the Arabian plate. AF: Alula-Fartaq fracture zone, CR: Carlsberg Ridge, GoS: Gulf of Suez, OFZ: Owen Fracture Zone. Red arrows represent GPS velocities from ArRajehi et al. (2010) and indicate counterclockwise rotation of the Arabian plate. **(b)** Timeline of main tectonic events in

the Red Sea-Afar-Gulf of Aden rift system (see text for details). GoA: Gulf of Aden, MER: Main Ethiopian Rift, MS: Magmatic segments. Modified after Zwaan et al. (2020a).

The Afar region is of further interest due to the occurrence of rotational rifting related to the anticlockwise pivoting of the Arabian plate (e.g. Smith 1993; Bellahsen et al. 2003; ArRahjehi et al. 2010, Fig. 1). A common simplification is namely that rifting involves constant along-strike extension conditions (e.g. Vink 1982). Yet in natural rifts deformation rates often change along-axis due to plate rotation about an Euler pole (e.g. Martin 1984; Van der Pluijm & Marshak 2004; Muluneh et al. 2013; Zwaan et al. 2020b). Recent analogue and numerical modeling studies show that such rotational plate motion strongly affects the development and allows propagation of rifting and continental break-up on regional to global scales (e.g. Molnar et al. 2017, 2018; Mondy et al. 2018; Zwaan et al. 2020b). The development of the Gulf of Aden and Red Sea rifts is a prime example, where extension rates double over every 1000 km (ArRajehi et al. 2010, Fig. 1, see section 1.2). The Afar region thus provides a unique natural laboratory to study the effects of rotational tectonics on rifting and passive margin development.

1.2. Geology of Afar

Afar forms a triangular depression near and partially below sea level, between the Ethiopian and Somalian Plateaux to the west and south, and the Danakil and Ashia Blocks to the NE and east (Figs. 1, 2). It is an area of highly extended crust, 25 km to 15 km thick from south to north, compared to the 40 km thick crust below the Ethiopian Plateau (Makris & Ginzburg, 1987; Hammond et al. 2011). From the north, the Red Sea rift axis steps into the Danakil Depression at the Gulf of Zula and extends to the SE through a number of offset rift basins. The Gulf of Aden rift axis enters Afar from the east at the Gulf of Tadjura (e.g. Makris & Ginzburg 1987; Manighetti et al. 1998, 2001). To the south and separated from the Red Sea and Gulf of Aden system by the Tendaho-Goba'ad Discontinuity (TGD), the Ethiopian Rift forms the third branch of the current Afar triple junction (Wolfenden et al. 2004).

The formation of the Afar Depression is associated with two large-scale processes: the rotation of the Arabian plate with respect to the Nubian/African plate and the emplacement of a thermal mantle anomaly beneath the continental lithosphere (Fig. 1b). Prior to rifting (40-30 Ma) a mantle plume is thought to have impacted the lithosphere below Afar (e.g. Rooney et al. 2017 and references therein). In Afar, this caused an intense flood basalt event at 30 Ma (Hoffman et al. 1997), the remains of which (Trap series) are found in large parts of Ethiopia and Yemen (e.g. Mohr 1983a; Bosworth et al. 2005, Fig. 1a). The outpouring of most of these basalt flows took place in ca. 1 Myr and covered the preceding Oligocene laterite surface with up to 2 km of volcanics (Mohr 1983a; Hoffmann et al. 1997; Abbate et al. 2015). Meanwhile, rifting started in the eastern parts of the Gulf of Aden at ca. 35 Ma (Leroy et al. 2010; Purcell 2017 and references therein) related to the counterclockwise motion of the Arabian plate about a rotation pole currently positioned near 31.7˚N 24.6˚E (McKenzie et al. 1970; Bellahsen et al. 2003; ArRajehi et al. 2010). Ongoing divergence of the Arabian plate caused rift propagation towards Afar around 26-31 Ma (Wolfenden et al. 2005; Ayalew et al. 2006) and subsequently to the Red Sea at ca. 23 Ma (Szymanski et al. 2016), creating a continuous L-shaped rift zone bordering the southern edges of the Arabian plate (Bosworth et al. 2005; Bosworth 2015). Oceanic spreading

in the easternmost Gulf of Aden was established around 17.6 Ma or even 20 Ma (Manighetti et al. 1997; d'Acremont et al. 2006; 2010; Fournier et al. 2010; Leroy et al. 2010), and reached the western Gulf of Aden around 10 Ma (Fig. 1a), whereas oceanization in the Red Sea started around 5 Ma (e.g. Bosworth et al. 2005; Cochran 2005; Augustin et al. 2014) or possibly as early as 12 Ma (Izzeldin 1987). Afar has however not reached complete break-up so far, reflecting a more complex local geological history (Fig. 1).

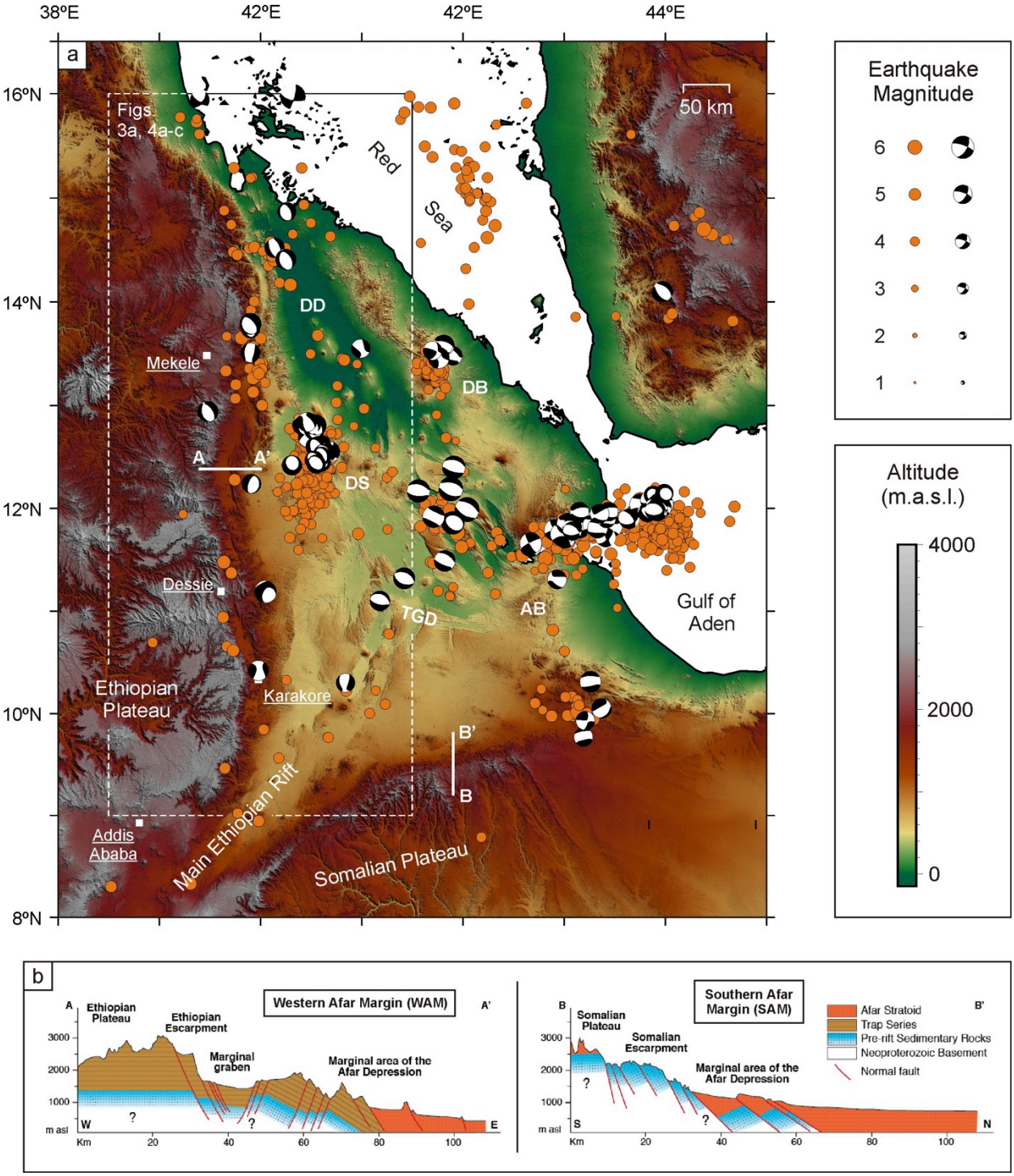

Fig. 2. (a) Afar Depression in East Africa and the location of the Western Afar Margin (WAM). Red dots indicate historic earthquakes from the 1970-2018 NEIC earthquake catalogue. Focal mechanisms are derived from the CMT catalogue. AB: Aisha Block, DB: Danakil Block. DD: Danakil Depression, DS: Dabbahu segment, TGD: Tendaho–Goba'ad Discontinuity. Topography is derived from ASTER data (90 m resolution). **(b)** Sections A-A' and B-B', illustrating the difference in structural style between between (A-A') the Western Afar Margin (WAM) and (B-B') the Southern Afar Margin (SAM). The former is dominated by antithetic faulting (towards the plateau) and associated marginal grabens, whereas the latter is characterized by synthetic (basinward) faulting. Section locations are indicated in (a). Image modified after Corti et al. (2015) and Beyene & Abdelsalam (2005).

The formation of the Southern Afar Margin (SAM) probably started at ca. 24 Ma (Bosworth et al. 2005, Fig. 2). Along the Western Afar Margin (WAM), rift-related volcanism and geomorphology indicates that extension simultaneously initiated in the north between 26-31 Ma and migrated to the south until 11 Ma (Zanettin & Justin-Visentin 1975; Wolfenden et al. 2005; Ayalew et al. 2006; Tesfaye & Ghebreab 2013). Around that time the Danakil Block, a continental sliver that was part of the stretched Red Sea/Afar rift zone (Morton and Black 1975; Collet et al. 2000; Redfield et al. 2003; Stab et al. 2016), started a counterclockwise rotation (Sichler 1980; Eagles et al. 2002; McClusky et al. 2010). This rotational motion is associated with the formation of the Danakil Depression, the current rift axis in northern Afar, which together with the parallel Red Sea trend forms a system of overlapping rift axes (Mohr 1972, Figs. 1a, 2). Simultaneously, the Aisha Block began a clockwise motion (Kidane 2015), possibly due to the propagating Gulf of Aden rift system. The northern part of the currently still continental Main Ethiopian Rift was formed around 11 Ma (Wolfenden et al. 2004; DeMets & Merkouriev 2016) due to the eastward motion of the Somalian plate with respect to the Nubian plate, and by linking up with the Red Sea and Gulf of Aden system, thus establishing the present Afar triple junction (Figs. 1a, 2).

At around 2 Ma deformation in Afar, which had over time gradually shifted from the rift margins into the depression, became strongly localized along narrow segments in the axial portion of the rift valley floor (e.g. Wolfenden et al. 2005). Here extension is accommodated primarily by episodic diking rather than pure faulting (e.g. Hayward & Ebinger 1996; Wright et al., 2006; Barnie et al., 2015; Medynski et al. 2016). These active magmatic segments, referred to as Axial Volcanic Ranges in Afar and Wonji Fault belt along the axis of the MER (e.g. Mohr 1967; Barberi et al. 1972; Dumont et al. 2019), create significant seismicity (Fig. 2a) and are considered to represent embryonic spreading centers heralding imminent break-up (e.g. Barberi et al. 1970, Barberi & Varet 1977; Ayelew et al. 2019).

Most recent scientific studies concerning Afar tend to focus on the development and interaction of the axial magmatic segments and the associated continental break-up processes (e.g., Dumont et al. 2019; Pagli et al., 2019). In contrast, the parts of Afar that represent (future) passive margins and thus provide unique research opportunities (i.e. the SAM and WAM, Fig. 2) receive relatively little attention, partially due to the often challenging geographical, climatological and political conditions in Ethiopia and Eritrea (e.g. Fazzini et al. 2015; Williams 2016; Varet 2018). The focus of this paper lies on the structural geology of the Western Afar Margin (WAM) and our aim is to provide an up-to-date detailed structural interpretation of the area by bringing

187 together data from previous publications, regional mapping, well logs, earthquake surveys and
188 recent fieldwork, and fitting these data in a regional tectonic framework.

189 1.3. The Western Afar Margin

190 The ca. N-S striking WAM represents a sharp transition in both topography and crustal thickness
191 from the Ethiopian Plateau to Afar over a distance of 50-100 km (Fig. 2). Altitudes on the
192 plateau reach as high as 4 km, whereas Afar lies near and even below sea level in the north.
193 Crustal thickness reduces from 40 km beneath the plateau to 25 km beneath southern and central
194 Afar and to 15 km beneath the Danakil Depression (Hammond et al., 2011).

195 The lithology of the WAM can be divided in six main units, separated by planation surfaces that
196 reflect the geological history of the Afar region (Abbate et al. 2015; Coltorti et al. 2015, Fig. 3a).
197 The oldest rocks are found in the north and belong to the Precambrian (Neoproterozoic)
198 metamorphic basement, containing a structural grain inherited from the Panafrican orogeny (e.g.
199 Drury et al. 1994; Collet et al. 2000; Ghebreab & Talbot 2000). Near the city of Mekele modest
200 occurrences of Paleozoic sandstones and glacial deposits occur (Arkin et al. 1971). The next unit
201 consists of Triassic Adigrat sandstones and Jurassic limestones that are abundant in the Mekele
202 basin (Arkin et al. 1971; Beyth 1972; Alemu et al. 2018). Cretaceous deposits are only
203 outcropping in the SW where the Blue Nile cuts deep into the Ethiopian Highlands (Kazmin
204 1972; Gani et al. 2007). At about 13˚N a distinct lithological divide occurs between the north,
205 where Precambrian-Jurassic units crop out, and the south, where Oligocene-Miocene Trap
206 basalts predominantly cover the Ethiopian Plateau and WAM. Patches of these lava flows are
207 also present in the north, suggesting that their pre-erosion extent was significantly larger (e.g.
208 Mohr 1983a; Mohr & Zanettin 1988). Extensive Miocene-present sedimentary and volcanic infill
209 (among which the Pliocene-Quaternary Stratoid units, Barberi & Santacroce 1980) forms the
210 most-recent unit and covers the Afar floor, but has also accumulated in depressions along the
211 WAM and on the Ethiopian Plateau (Fig. 3a).

212 The structural style of the WAM is characterized by a number of notable features. Firstly,
213 faulting along the margin is generally considered to be dominantly antithetic (i.e. dipping away
214 from the Afar rift basin) (e.g. Abbate & Sagri 1969; Baker et al. 1972; Mohr 1983a; Wolfenden
215 et al. 2005; Stab et al. 2016, Fig. 2b). As a result, fault blocks seem to be increasingly tilted
216 towards Afar as indicated by increasing dips of the Trap basalt layers and rotated dikes, in a
217 system which has been described as “flexure” of the crust into Afar (Abbate & Sagri 1969).
218 Furthermore, a series of faulted basins, referred to as “marginal grabens” (Mohr 1962) align
219 along the WAM (Figs. 2, 3). These grabens, (partially) filled with Pliocene-Recent sediments
220 (Chorowicz et al. 1999; Abbate et al. 2015), are associated with the dominant antithetic style
221 faulting, a situation that is in contrast to the SAM and Yemen margin, of which the bordering
222 plateaus have very similar altitudes, but faults are considered to be dominantly synthetic (i.e.
223 dipping basinward, Baker et al. 1972; Berhe 1985, 1986; Beyene & Abdelsalam 2005, Fig. 2b).
224 Where antithetic faulting occurs along the SAM or Yemen, no marginal grabens have developed
225 (Berhe 1985, 1986; Tesfaye et al. 2003; Davison et al. 1994, 1998; Geoffroy et al. 1998).
226 Terminology and toponymy in the area is often confusing since authors regularly use different
227 names and spelling, due to changing political realities and the difficulties in translating local
228 names in Latin script (Gouin 1979; Williams 2016). In this work we follow and refine the

marginal graben nomenclature established by Zwaan et al. (2020a) (Fig. 3b, see also the supplementary material: Zwaan et al. 2020c).

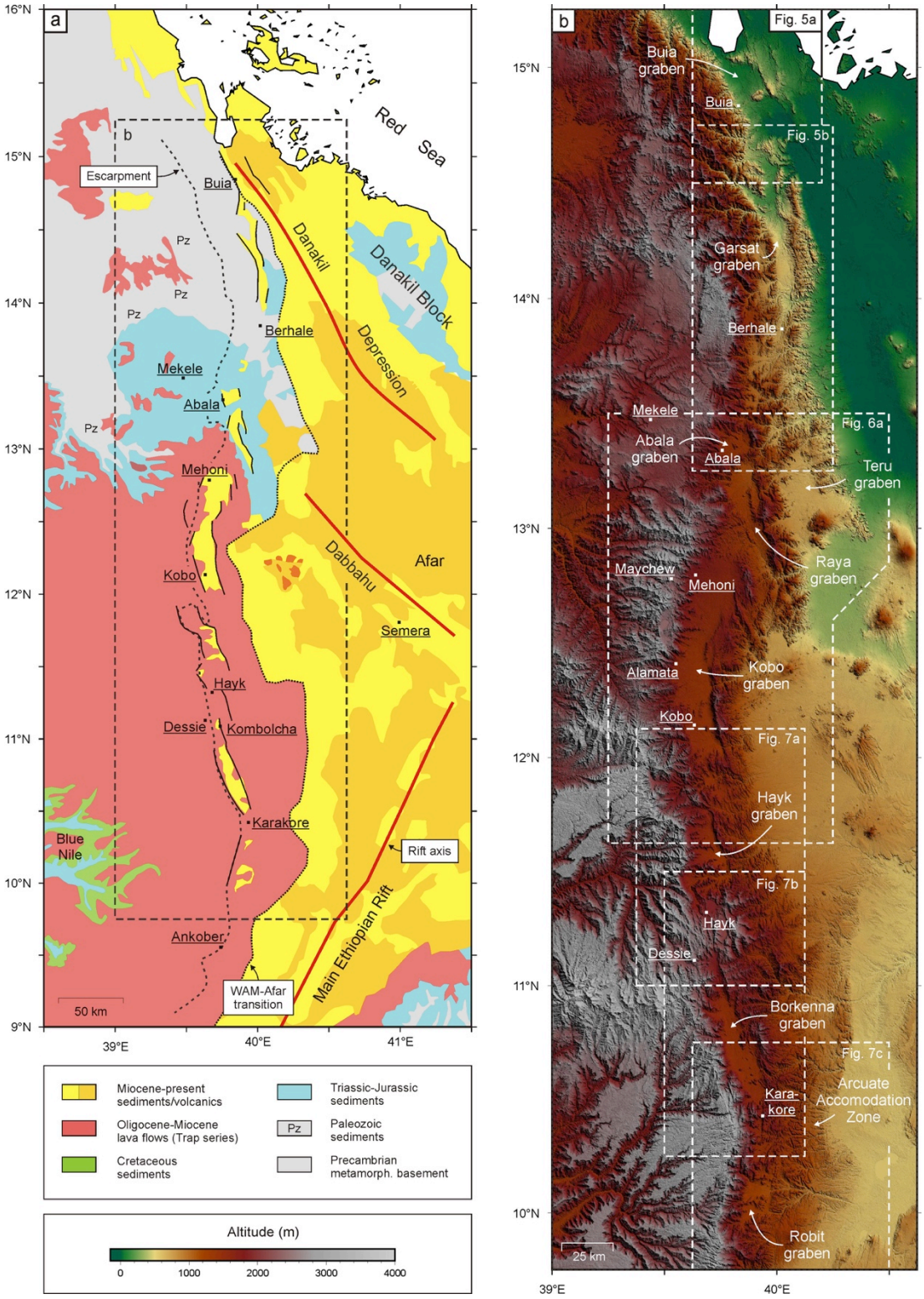

Fig. 3. (a) Geological map of the WAM. Modified after Arkin et al., 1971; Kazmin (1972), Barberi et al. (1972) and Kazmin et al. (1978). **(b)** Distribution of marginal grabens along the Western Afar Margin (WAM). The dotted boxes indicate the locations of detailed maps presented in Figs. 5, 7-9.

Another important feature is the presence of ongoing seismic activity along the WAM. Most earthquakes in the region are concentrated along the rift axes of the Red Sea, Gulf of Aden, central Afar and the MER (e.g. Tesfaye & Ghebreab 2013, Illsley-Kemp et al. 2017; 2018a, b, Fig. 2a). Some minor activity is registered at the SAM as well, but a significant proportion of the region's seismicity is recorded along the whole of the WAM (e.g. Gouin 1970, 1979; Hofstetter & Beyth 2003; Ayele et al., 2007; Craig et al., 2011; Goitom et al., 2017; Illsley-Kemp et al., 2018a, Fig. 2a). Historical accounts describe devastating earthquakes along the margin and as recent as 1961 a series of earthquakes with magnitudes up to 6.4 struck Korakore, causing significant damage in the area (Gouin 1979, Fig. 2a). The ongoing activity shows that WAM is not a true passive margin yet (Corti et al. 2015; Zwaan et al. 2020a).

2. Methods

We use three different approaches in order to obtain new data for an integrated structural interpretation of the WAM and adjacent parts of Afar, involving (1) analysis of earthquake datasets to quantify current deformation in the region, and to characterize active faults, (2) large-scale structural mapping by means of geomorphological analysis, and (3) new field data as well as unique well logs collected at key locations in the study area to verify and refine the structural interpretation. These methods are described in more detail below and extensive supplementary material is publicly available in the form of a GFZ Data Publication (Zwaan et al. 2020c).

2.1. Seismicity analysis

Earthquake data helps to visualize ongoing tectonic activity in the area. We consider data from various sources. Firstly, the National Earthquake Information Centre (NEIC) catalogue (849 earthquakes since 1973, https://earthquake.usgs.gov) which is complete above magnitudes of ca. M4, and hypocenter positions have error bars of ca. +/- 20 km. We combine the NEIC catalog with focal mechanism data (99 events from the Global Centroid Moment Tensor (CMT) Catalog (Dziewonski et al. 1981; Ekström et al. 2012, https://www.globalcmt.org), to obtain a coarse impression of the large-scale tectonics in Afar (Fig. 2).

For more detailed analysis we use high-resolution data from the study area. We use the local earthquake catalogues from Ebinger et al. (2008), Keir et al. (2006, 2009) (Belachew et al. (2011), and Illsley-Kemp et al. (2018a) with a total of 13499 events from the period 2001 -2013. These catalogs together provide coverage of large parts of the WAM with a magnitude of completeness of a little above M_L2, and were used to compute spatial variations in seismic moment release (SMR) of the area. Furthermore, the extraction of T-axes using earthquake focal mechanisms from the NEIC catalog as well as the Keir et al. (2006) and Illsley-Kemp et al. (2018a, b) surveys provides an insight of ongoing fault slip style and direction.

In order to better resolve the locus of faulting and subsurface fault geometry of the WAM we used the earthquake datasets of Belachew et al. (2011) and Illsley-Kemp et al. (2018a). To homogenize our earthquake dataset, we relocated the Belachew et al. (2011) catalog using NonLinLoc and the same velocity model as used in Illsley-Kemp et al. (2018a). From this now standardized and combined dataset, we use a selection of 3689 earthquakes with epicenter location error bars of +-5 km or less in three dimensions (xyz) for subsequent structural analysis plotted in both map and section view using Generic Mapping Tools (GMT, http://gmt.soest.hawaii.edu/).

2.2. Structural mapping

Mapping of the structures within the study area was predominantly carried out through geomorphological analysis in QGIS (www.qgis.org). Detailed (30 m resolution) Shuttle Radar Topography Mission (SRTM) and Advanced Spaceborne Thermal Emission and Reflection Radiometer (ASTER) digital topography data from NASA and METI (https://earthexplorer.usgs.gov) provide an excellent basis for structural mapping, especially due to the dry climate preserving fault-related topography in the area (e.g. Chorowicz et al. 1999; Fazzini et al. 2015). Satellite images and the possibility to observe these in 3D in Google Earth Pro allow additional quality control and the identification of other features such as dikes and tectonic lineaments. Criteria for a proper fault interpretation include the presence of layering in the hanging wall, the general shape of tilted fault blocks, and the apparent presence of a fault plane. Especially the pre-rift Trap basalts are of great interest, as they provide a pre-rift sub-horizontal reference that allows us to recognize syn-rift deformation.

2.3. Field and well data collection

A recent field campaign along the WAM provided a crucial opportunity to ground truth the large-scale structural interpretation acquired through the methods described in sections 2.1 and to gain further insights in the associated tectonic regime. Since fault measurements are available from the northernmost (Buia, Sani et al. 2017) and the southern sections of the margin, (Robit, and Borkenna, Chorowicz et al. 1999) we focused our efforts on the central part of the WAM, between Berhale to the north to the Karakore fault in the south (Fig. 3b). We visited various key locations, i.e. outcrops along interpreted faults, to collect fault data (fault strike, dip direction, pitch and sense of fault slip). Additional field data was collected during a second campaign in the northernmost WAM in Eritrea, where N-S trending faults offsetting the Dandiero basin sedimentary infill were measured. Analysis of fault data with Wintensor (Delvaux & Sperner 2003) was performed in order to determine fault characteristic and the stress field under which they developed

Furthermore, the first-order geomorphological observations made along the margin during both field campaigns are highly valuable for assessing fault activity. We also collected unique well logs from irrigation projects near the towns of Mehoni, Alamata and Kobo in the agriculturally important Kobo graben (Tadesse et al. 2015; Zwaan et al. 2020c, Fig. 3) that allow the construction of the first-ever borehole-calibrated structural profiles of the WAM.

3. Large-scale earthquake analysis

3.1. Earthquake distribution and seismic moment release (SMR)

Plotting all available data from the Keir et al. (2006), Belachew et al. (2011) and Illsley Kemp et al. (2018a) earthquake catalogues, shows intense seismic activity along the rift axes in Afar (Fig. 4a). Here a distinct right-stepping zigzag pattern emerges, connecting the Danakil rift axis to the north with the Dabbahu segment to the south, perhaps marking structures that transfer strain between both rift axes (e.g. Dumont et al. 2019). Less continuous patches of recorded earthquakes to the south indicate the location of the MER (Fig. 4a). Note however, the significant number of seismic events along the sigmoidal trace of the whole WAM, which are most concentrated between ca. 12.5N˚-14˚N (Fig. 4a).

Although a lower number of earthquakes are recorded in the southern sectors of the WAM due to a lack of seismic stations there, the calculated seismic moment release (SMR) does not show a significant decrease in energy (Fig. 4b). This is consistent with the fact that some of the major earthquakes in (recent) Ethiopian history occurred in the southernmost sectors of the WAM, near Ankober and Karakore (Gouin 1979, Fig. 2b). We also clearly observe a high concentration of seismic moment release along the various rift axes in Afar (Fig. 4b). Calculations by Illsley-Kemp et al. (2018a) have shown that these account for 2/3 of the energy release in the Danakil rift axis, whereas the WAM takes up the remaining third in the region north of 12.5˚N. Our data now confirms this distribution for the whole WAM.

3.2. Tectonic stress calculation from focal mechanisms

Earthquakes are a manifestation of a region's tectonic stress field. However, the non-linear interaction between the stress field and frictional slip on fault planes mean it is difficult to draw inferences regarding stress field orientation from individual earthquake focal mechanisms. We separate focal mechanisms from Keir et al. (2006), Illsley-Kemp et al. (2018a, b), and the CGMT database, into geographically distinct regions. We then use a Bayesian method of stress parameter estimation (Arnold & Townend, 2007), which accounts for errors in nodal plane parameters, to infer tectonic stress parameters for each region. This provides us with a quantitative measure of the current extension direction along the WAM and the adjacent Afar (Fig. 4c). The WAM north of 10.5˚N is characterized by a ca. WSW-ENE extension, of which the cluster east of Mekele provides a statistically significant mean S_3 strike of 82˚N (Fig. 4c, d). South of 10.5˚N, the S_3 orientation indicates an east-west extension near Karakore, and a more WNW-ESE extension where the margin aligns with the MER. Here, S_3 has a statistically significant mean trend of 108˚E (Fig. 4c, d). At the Dabbahu segment and along the Danakil rift axis in Afar, extension is slightly more to the NE (66˚N) compared to the WAM (mean extension direction: 82˚N, Fig 4c, d), which is in agreement with the ca. 60˚N extension at the Danakil axis reported by La Rosa et al. (2019).

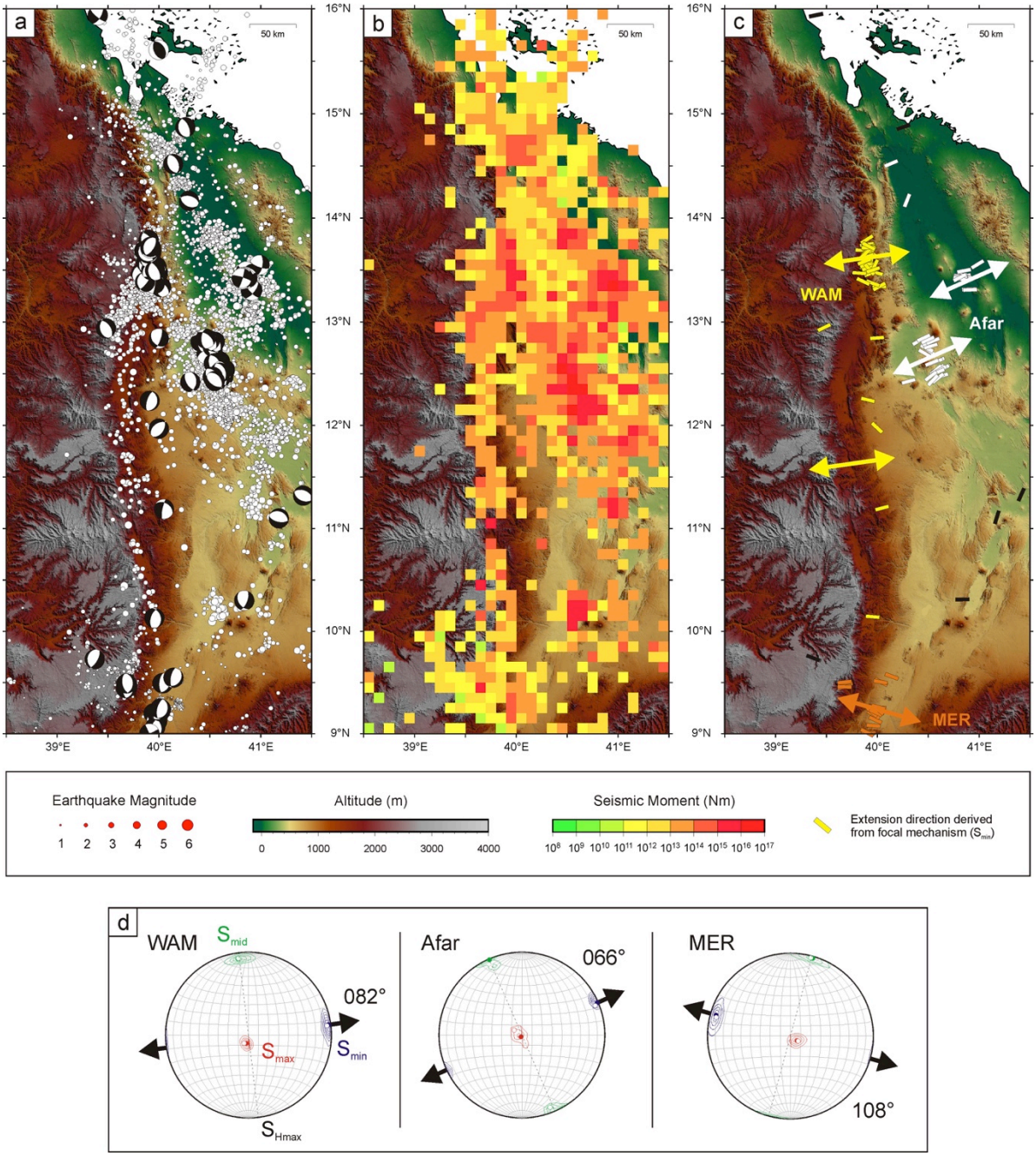

350

351 **Fig. 4.** Large-scale earthquake analysis. **(a)** Map of combined earthquakes from the Keir et al.
352 (2006), Belachew et al. (2011) and Illsley-Kemp et al. (2018a) datasets (survey periods: 2001-
353 2003, 2007-2009 and 2011-2013, respectively). Focal mechanisms are from the CMT database,
354 Keir et al. (2006) and Illsley-Kemp et al., (2018a, b). **(b)** Seismic moment release (SMR) map of
355 the WAM and nearby Afar, produced with the earthquake data presented in (a). **(c)** Tectonic
356 stress parameters revealing current extension directions along the Western Afar Margin (WAM),
357 Afar and Main Ethiopian Rift (MER) derived from the earthquake focal mechanisms presented
358 in (a). The general results of the calculation are shown in **(d)**. Background topography is derived
359 from ASTER data (90 m resolution). Map locations shown in Fig 2a.

4. Structural mapping

Detailed maps of every marginal graben area are presented in Figs. 5-7, we show the results of detailed earthquake-based fault interpretation in Fig. 8, and a general overview of interpreted faults along the WAM are provided in Fig. 9a, b. The main points of this mapping effort are laid out below, but an exhaustive description of the characteristics of the WAM is made available in the supplementary materials (Zwaan et al. 2020c).

4.1. Fault and marginal graben trends

Although the WAM is aligned north to south, the numerous normal faults we mapped along the margin display a dominant NNW-SSE strike (Figs. 5-7, 9a, d). The exception to this is the southernmost part of the WAM, below ca. 10.5˚N, which shows clear fault realignment with the NNE-SSW striking Main Ethiopian Rift (Figs. 7b, c, 9a). Naturally, the marginal grabens follow the same trends, and the discrepancy between the general fault alignment and the WAM orientation is accounted for by the presence of various accommodation zones between the marginal grabens. These accommodation zones come in different forms. A minor but well-defined NNE-SSW graben (Dandiero basin) forms the connection between the Buia and Garsat grabens (Fig. 5a, b). By contrast the latter is linked to the Abala graben through a NNE-SSW area of rather chaotic topography (Fig. 5b). Between the Abala, Raya, Teru and Kobo grabens lie various ridges with different orientations (Fig. 6a). The Teru graben represents an anomaly in that it opens into Afar and somewhat out of sync with the general right-stepping arrangement (Fig. 6a). The northern part of the Hayk graben diverts towards the west, away from the Kobo graben into the Ethiopian plateau, creating a type of overlapping graben zone (Fig. 6a). To the south, the Hayk graben transitions into the complex Desi-Bati Accomodation Zone through which it links with the Borkenna graben (Fig. 7a, b). The latter at its southern tip sees the faults diverting to N-S and then NNE-SSW over the Arcuate Accomodation Zone that connects the WAM with the Main Ethiopian Rift (Tesfaye et al. 2003, Fig. 7b). Here, a second set of faults follows an opposite curve from SSW-NNE to NNW-SSE, giving an “hourglass” shape in map view, possibly marking the initial location of the SW tip of the Arabian Peninsula before Afar rifting (Tesfaye et al. 2003). This transition from the Borkenna to Robit graben through the Arcuate Accomodation Zone is rather gradual (Fig. 7c-d).

The type of faulting we observe by means of topography analysis is in general agreement with previous concepts, i.e. synthetic escarpment faults west of the marginal grabens and numerous antithetic faults and small tilted fault blocks to their east (Figs. 2b, 5-7, 9). The latter are however much better defined in the southern parts of the WAM, where the Trap basalts are preserved (Fig. 3a). In the northern areas (Buia to Raya/Teru grabens), where these basaltic units are removed by erosion (Mohr 1983a; Bosworth et al. 2005), no clear pervasive antithetic faulting is observed (Figs 5, 6a).

4.2. Constraints on recent fault activity

Fault morphology provides an impression of fault activity, as fresh, uneroded fault scarps indicate recent displacement, which we complement with detailed seismicity analysis using earthquake data with <10 km hypocenter error margins, as well as information form boreholes. In the Buia graben, both the western and eastern boundary faults are well-defined (Fig. 5a), where the former displaces large Quaternary fan systems (Abbate et al. 2004; Sani et al. 2017).

The clear slope breaks along the Garsat graben indicating recently active faults (Fig. 5b), although the nature of the eastern graben edge is elusive (fault or sedimentary contact? Fig. 5c). No field measurements are available due to the highly erodible schisteous lithology characterizing the basement units (Barberi et al. 1972; Kazmin 1972, 1978, Fig. 3a). Well-localized earthquake data in the northernmost part of the WAM (Buia-Garsat) are limited and concentrated along the Danakil axis.

The chaotic zone separating the Garsat and Abala grabens, as well as in the Abala graben itself contain sufficiently concentrated high-quality earthquake data for detailed fault interpretation (Fig. 8a). We plot the events on E-W sections (Q1-5, Fig. 8), projecting seismicity from 3 km either side of the profile (Fig. 8a). The plots reveal seismicity defining a number of antithetic faults, yet these faults are not always associated with the apparent rift boundary faults in the area (Figs. 8b-f). Our analyses improve upon previous interpretations (Illsley-Kemp et al., 2018a) and better define the active antithetic fault systems. Section Q1 shows an antithetic fault that may be the eastern boundary fault of the small Wikro graben, as well as some other minor antithetic faults (Fig. 8a, b). Also section Q2 shows clear antithetic faulting, potentially a continuation of the Wikro Graben Fault from Q1 (Fig 8a, b). More to the south in section Q3, the Wikro Dike Swarm seems inactive, yet a possible antithetic fault occurs east of it (Fig. 8d), representing a southward continuation of the Wikro Graben seismicity into the zone east of the Abala graben (Fig. 8a), also seen in section Q4 (Fig. 8e). Section Q4 captures the East Abala Fault, which is aligned with the dominant eastern boundary fault of the Raya graben to the south (Fig. 5b, 6a, 8a). The last section (Q5) reveals antithetic fault activity at the Abala-Raya Ridge (Fig. 8a, f), which is however not clearly associated with a surface fault.

A belt of seismicity is projected to the SW from the Abala-Raya Ridge (Figs. 6a, 9c), possibly indicate a reactivated basement structure of perhaps Pan-African origin (e.g. Ghebreab & Talbot 2000). Just to the south of this earthquake zone, the northern Kobo sedimentary plain is bordered by a series of rather well-developed eastern boundary faults, whereas a strongly eroded margin occurs in the west (Fig. 6a). Yet the significant and linear topographic downstep at the western edge of the northern Kobo plain implies an important, but recently inactive normal fault (Mehoni Fault). Instead, a major active fault system (Maychew Fault) occurs on the plateau to the west, forming the current western boundary fault of the northern Kobo marginal graben structure, which has “stepped back” into the plateau and continues southward to the small Hashenge basin. (Fig. 6a). The westward shift of earthquake activity just to the north of the Kobo graben fits well with the prominence of the Maychew Fault (Fig. 6a, 9c). Borehole-controlled section S3 (Fig. 6a-c) shows both the Maychew and Mehoni fault in the west, as well as sedimentary infill thickening towards the east (122 m in well BH-2 and 222 m in well PZ-1), interrupted by the northern extension of the Bariye Fault (Figs. 6b, c). In the east the 198 m deep well BH-1 does not reach bedrock, and also registers geothermal activity, possibly related to recent faulting. This indicates that deformation is not localized along a single fault in this part of the margin.

In the southern Kobo graben, the scarce seismicity data seems to shift to the prominent East Kobo Fault, whereas its western counterparts are poorly defined (section S4, Fig. 6a, d, 9c). Wells near Alamata suggest limited (ca. 100 m) sediment infill there, whereas PK3-5, and TK1(RE) near Rare indicate thicker deposits toward the east (Fig. 6a, b). A second structural profile (S4, Fig. 6d) south of Kobo town describes a similar trend with well TK6 indicating a fault step similar to the one in Section S3 (Figs. 6c, d). We have no direct data in the east, but

446 based on geomorphology (depocenter location, Billi et al., 2015) and data from the wells near
447 Rare, the thickest deposits should occur near the East Kobo Fault (Fig. 6b), which likely has
448 accommodated most of the recent deformation in the area.

449 Seismic data south of the Kobo graben is too scarce for proper analysis, but the boundary faults
450 of the northern Hayk basin are well-defined as they cut into the Ethiopian plateau, indicating
451 ongoing activity (Fig. 7a). The depocenters near the antithetic Mersa Fault and its pronounced
452 morphology imply recent deformation as well. Further south towards the Dessie-Bati
453 Accomodation Zone, numerous well-defined faults are present, suggesting a complex active
454 deformation (Fig. 7a, b). In the Borkenna area, the antithetic eastern boundary faults are marked
455 by clear slope-breaks, suggesting ongoing deformation, whereas the Kolemo Fault to the west
456 looks rather eroded (Fig. 7b). Yet the Western Borkenna Fault is rather well-defined, as are its
457 equivalents to the south (Ataye and Ankober Faults, Fig. 7b, c). Finally, the Karakore Fault,
458 responsible for the 1961 Karakore seismic crisis (Gouin 1979), represents the main antithetic
459 fault in the Arcute Accomodation Zone (Fig. 7b-d).

460 Geomorphological interpretation supported by detailed earthquake analysis and well data thus
461 suggests some variation in the location of the currently dominant boundary faults in the marginal
462 grabens (i.e. antithetic vs. synthetic graben boundary faults, Fig. 9a), yet the large and sudden
463 topographical decline along the whole of the margin (i.e. the escarpment, Fig. 3) implies an
464 continuous synthetic boundary fault system that has accommodated significant, km-scale
465 deformation over time, even if segments of it are currently inactive and partially eroded. By
466 comparison, the offsets of the recently active eastern boundary faults are much smaller, and those
467 of the pervasive antithetic faulting small to minimal.

468 4.3. Additional observations

469 Between the Garsat and Abala graben, a N-S series of dikes (Wikro Dike Swarm) occurs, which
470 transitions in the East Abala Fault (Fig. 5a). Within the Kobo-Hayk Accomodation Zone, a series
471 of ca. SW-NE Miocene dikes (Stab et al. 2016) interrupt the general NNW-SSE fault architecture
472 (Fig. 6a). Chorowicz et al. (1999) suggest a relation between the latter dike family and the
473 formation of the northern MER, around 11 Ma (Wolfenden et al. 2004, DeMets & Merkouriev
474 2016 and references therein), causing a short phase of ca. NW-SE extension in the area (see also
475 section 6.3).

476 Furthermore, we observe that the floor of most grabens is rather irregular and interrupted by
477 prominent ridges and tilted fault blocks (Figs. 5-7). This is likely due to the basins being
478 underfilled as confirmed by our borehole data from the Kobo graben, which forms the largest
479 sedimentary basin along the WAM, revealing marginal graben infill of not more than a couple of
480 hundred meters thick (Fig. 6c, d, Zwaan et al. 2020c). The Buia graben with up to 500 m of
481 sediments forms an exception, but is not a marginal graben *sensu stricto* since it forms
482 continuation of the Danakil rift axis (Sani et al. 2017; Zwaan et al. 2020a, Fig. 5a). Indeed, we
483 observe various rivers that cross-cut the margin, draining the marginal grabens and even eroding
484 their limited sedimentary infill (Billi 2015), so that instead of filling available accommodation
485 space, material is directly transported to the main depocenter in Afar proper. As a result, the
486 extent of sedimentary basins or plains is not always equivalent to the actual marginal graben

structure (e.g. the Hayk graben structure is much larger than its sedimentary plains seems to suggest; Fig. 7a).

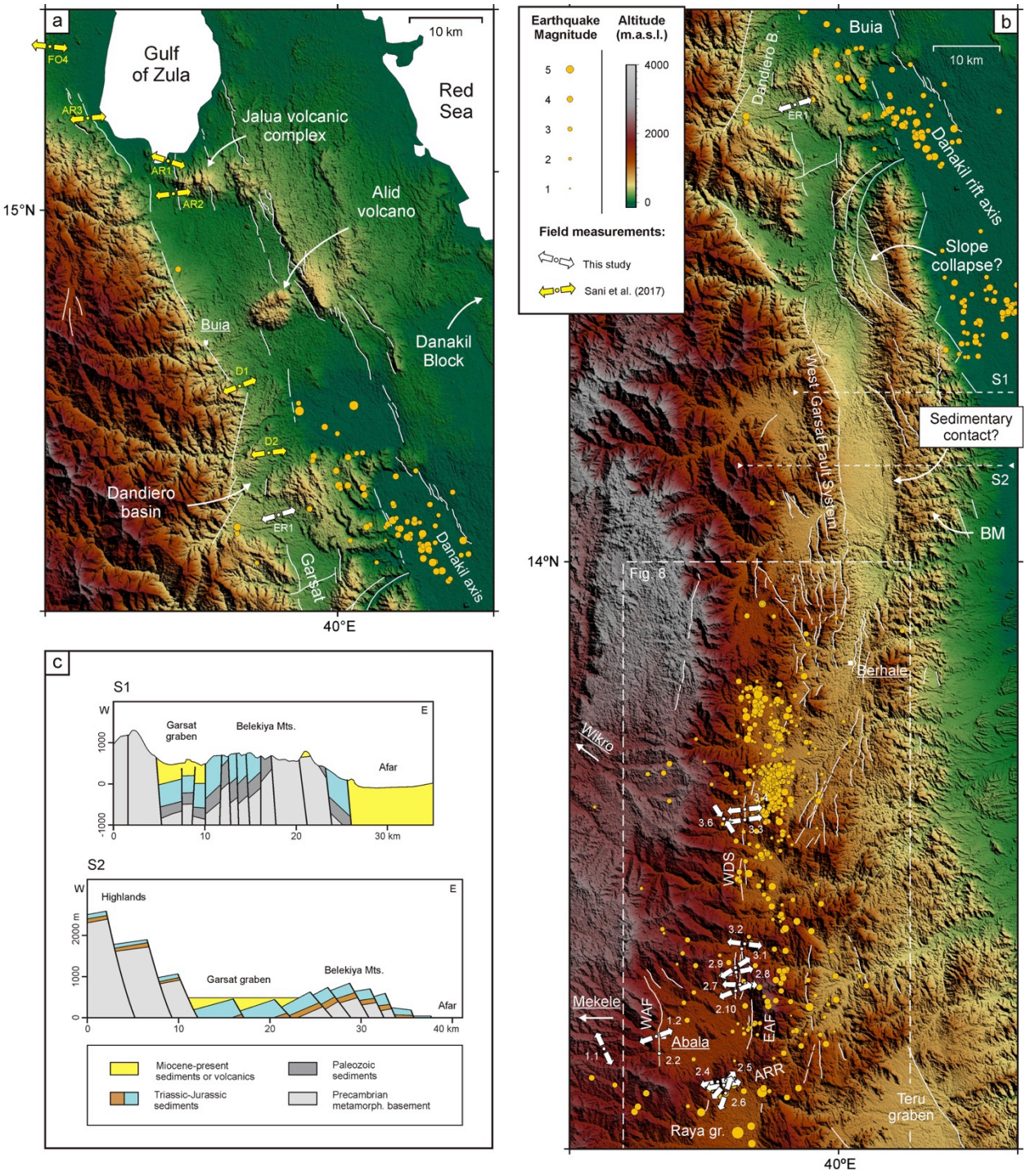

Fig. 5. Detailed maps of **(a)** the Buia graben and **(b)** Garsat graben. AAR: Abala-Raya Ridge, EAF: East Abala Fault, BM: Belekiya Mountains, WAF: West Abala Fault, WB: Wikro Basin WDS: Wikro Dike Swarm. Note the crescent-shaped depression at NE edge of the Garsat graben, which Chorowicz et al. (1999) interpret as a slope collapse structure. Earthquakes are shown by

yellow circles, scaled for magnitude, interpreted faults by white lines. Background topography is derived from ASTER data (90 m resolution). For locations, see Fig. 3b. **(c)** Two contrasting structural interpretations for the SE Garsat graben margin, S1 being the interpretation by Kazmin et al. (1978) involving a faulted contact, whereas Williams (2016) proposes a halfgraben architecture with a sedimentary contact on the basis of data from Garland 1980 (S2). Hagos et al. (2016) and Le Gall et al. (2018) support the latter option. (Approximate) section locations are indicated in **(b)**.

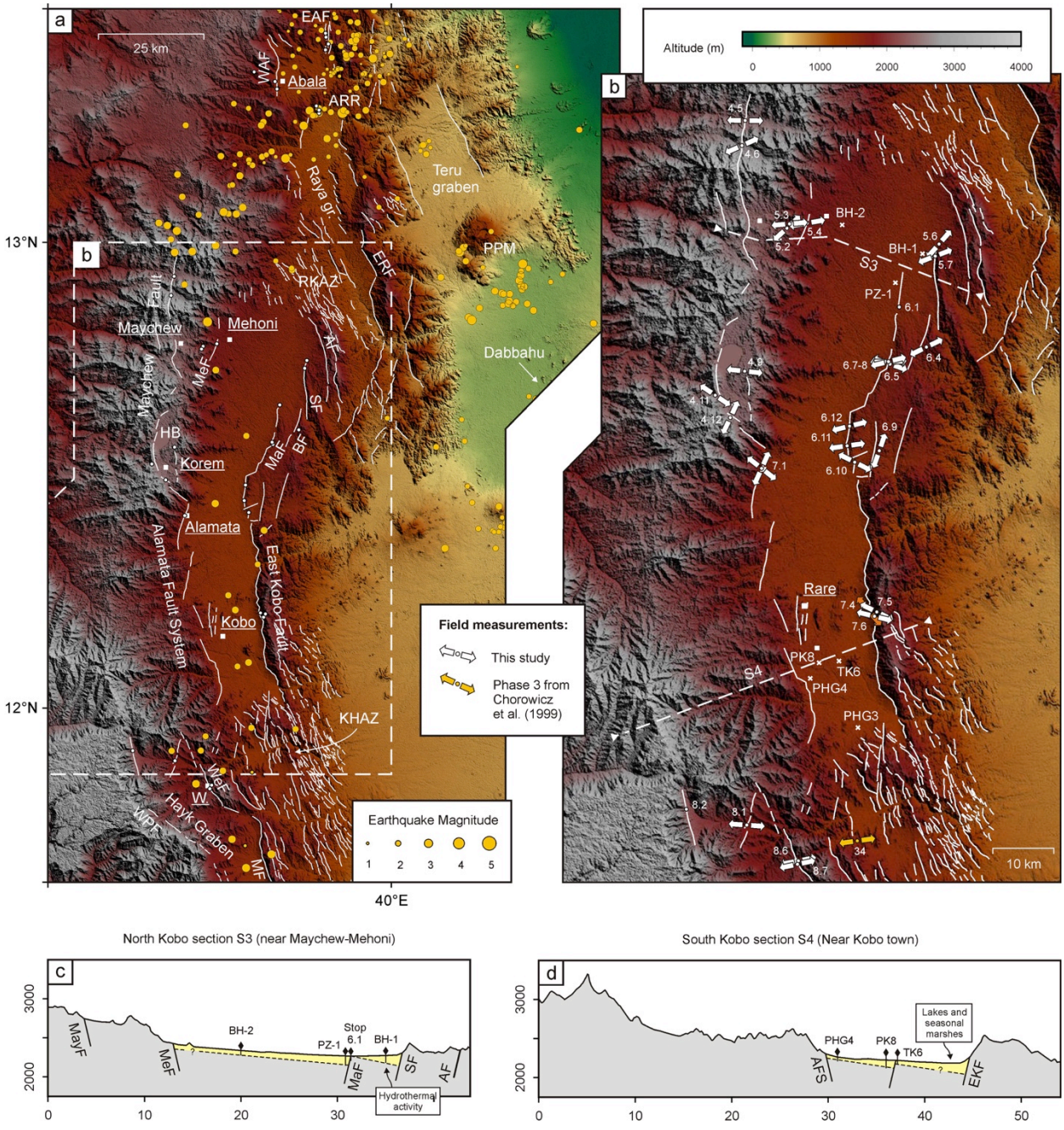

Fig. 6. Detailed maps of **(a)** Kobo-Raya-Teru area and **(b)** zoom in on the Kobo graben. AF: Abdera Fault, ARR: Abala-Raya Ridge, AsB: Ashenge basin, BF: Bariye Fault, EAF: East Abala

Fault, KHAZ: Kobo-Hayk Accommodation Zone, MaF: Manu Fault, MeF: Mehoni Fault, MF: Mersa Fault, PPM: Pierre Pruvost Massif, RKAZ: Raya-Kobo Accommodation Zone; SF: Solaka Fault, W.: Weldiya (town), WAF: West Abala Fault, WeF: Weldiya Fault, WPF: West Plateau Fault. Earthquakes are shown by yellow circles, scaled for magnitude, interpreted faults by white lines. Background topography is derived from ASTER data (90 m resolution). For location, see Fig. 3b. **(c, d)** Well-controlled sections S3 and S4 through the northern and southern sectors of the Kobo graben, respectively. See **(b)** for well locations, indicated by crosses. Well data are provided in the supplementary materials (Zwaan et al. 2020c).

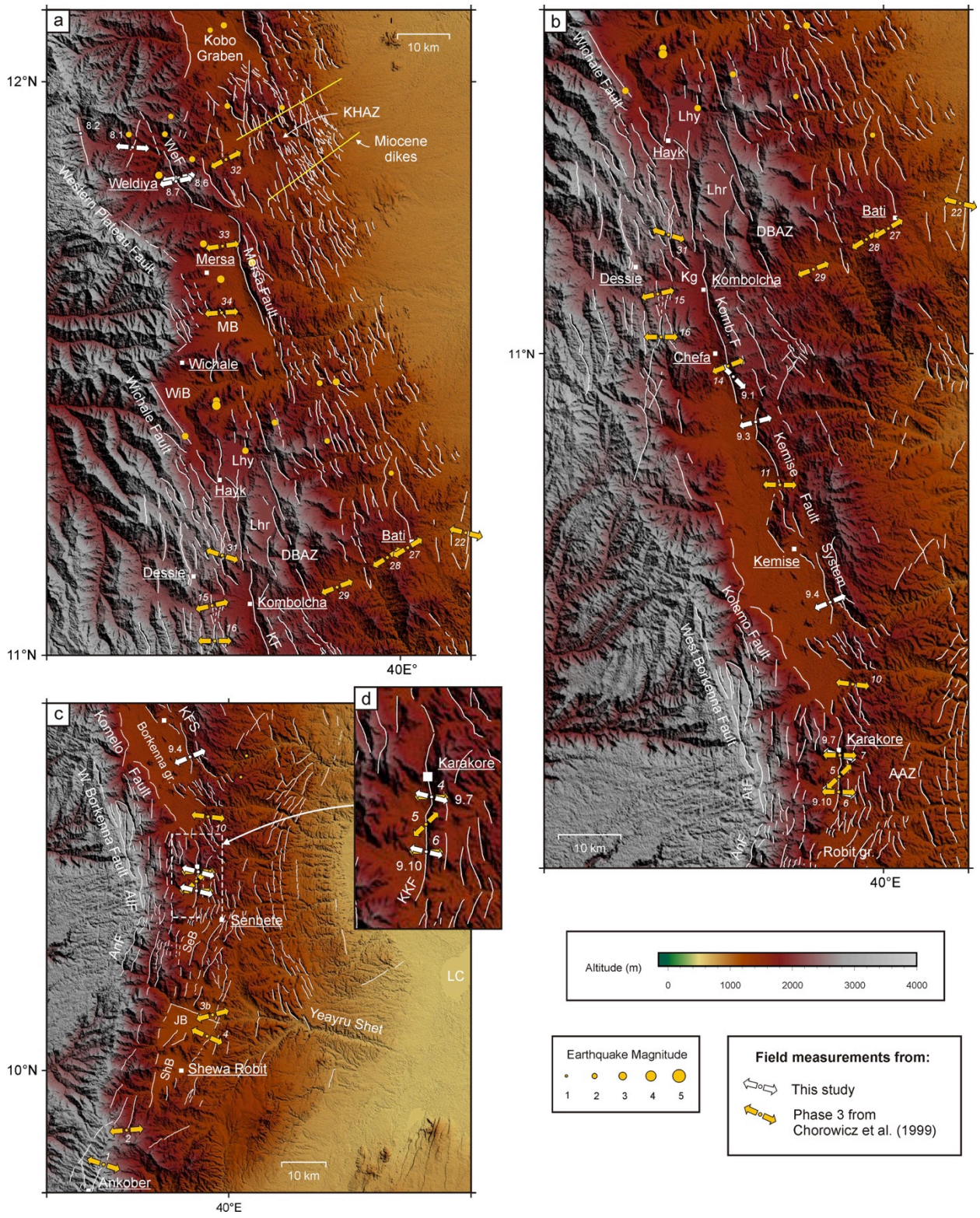

Fig. 7. Detailed maps of **(a)** the Hayk graben area, **(b)** the Borkenna graben and **(c)** the Arcuate Accomodation Zone and Robit graben. AAZ: Arcuate Accommodation Zone, AtF: Ataye Fault, AnF: Ankober Fault, DBAZ: Dessie-Bati Accommodation Zone, Kg: Kombolcha graben,

KHAZ: Kobo-Hayk Accommodation Zone, KKB: Karakore basin, KF: Kombolcha Fault, KKF: Karakore Fault, LC: Lake Caddabassa, Lhr: Lake Haribo, LHy: Lake Hayk, MB: Mersa basin, SeB: Senbete basin, ShB: Sheba basin, WiB: Wichale basin. Earthquakes are shown by yellow circles, scaled for magnitude, interpreted faults by white lines. For location, see Fig. 3b.

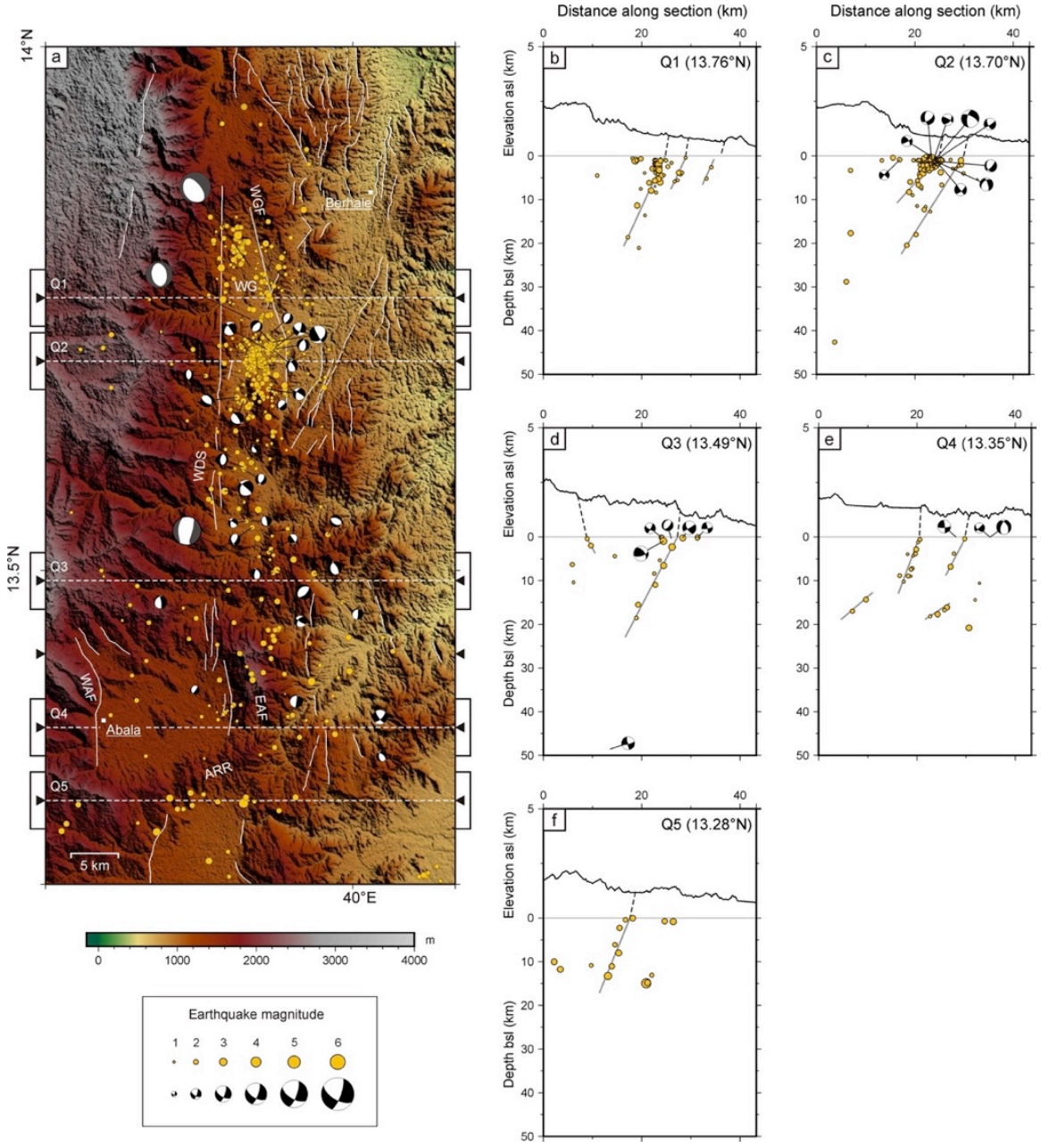

Fig. 8. (a) Detailed analysis of the southern Garsat basin/Wikro graben area. Earthquakes shown are a selection from the Illsley-Kemp (2018a) seismic survey and relocated dataset from Belachew et al. (2018) (selection criteria: xyz error margins ≤ 10 km). Grey focal mechanisms are derived from the CMT dataset, the black focal mechanism from the Illsley-Kemp et al. (2018a) catalogue. ARR: Abala-Raya Ridge, EAF: East Abala Fault, WAF: West Abala Fault, WDS: Wikro Dike Swarm, WG: Wikro graben, WGF: Wikro graben Fault. Earthquakes are

528 shown by yellow circles, scaled for magnitude, interpreted faults by white lines. **(b-f)** Five E-W
529 sections (Q1-5) showing earthquake clusters indicating active faults (grey lines) and how these
530 may relate to faults visible at the surface (dotted lines). Earthquake swoop width is 6 km as
531 indicated by the boxes on both sides of the map. For location, see Fig. 5b. Topography is derived
532 from ASTER data (90 m resolution).

533

534

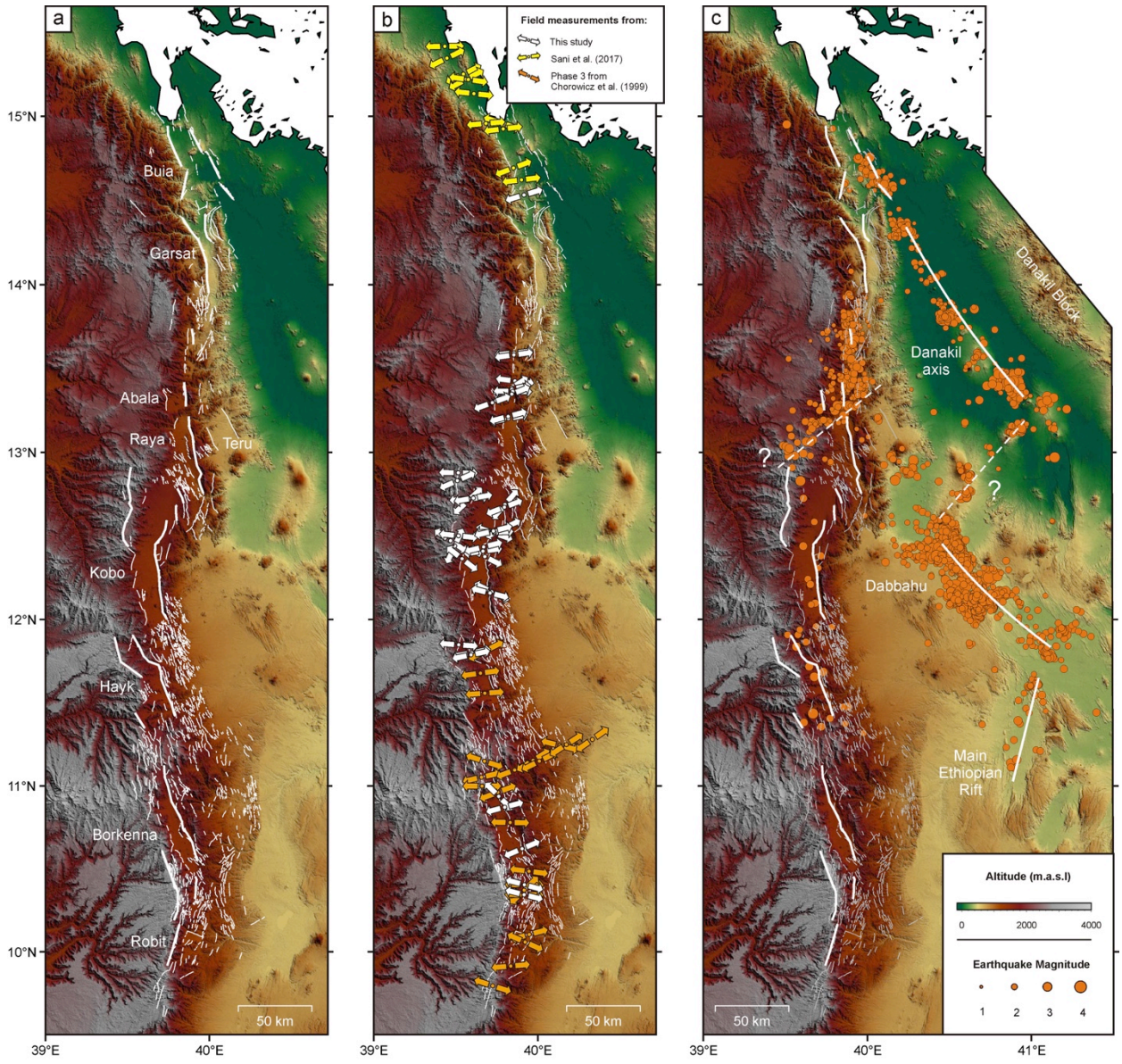
a
b
c
Field measurements from:
This study
Sani et al. (2017)
Phase 3 from Chorowicz et al. (1999)
Buia
Garsat
Abala
Raya
Teru
Kobo
Hayk
Borkenna
Robit
Danakil Block
Danakil axis
Dabbahu
Main Ethiopian Rift
Altitude (m.a.s.l)
0
2000
4000
Earthquake Magnitude
1
2
3
4
50 km
15°N
14°N
13°N
12°N
11°N
10°N
39°E
40°E
41°E

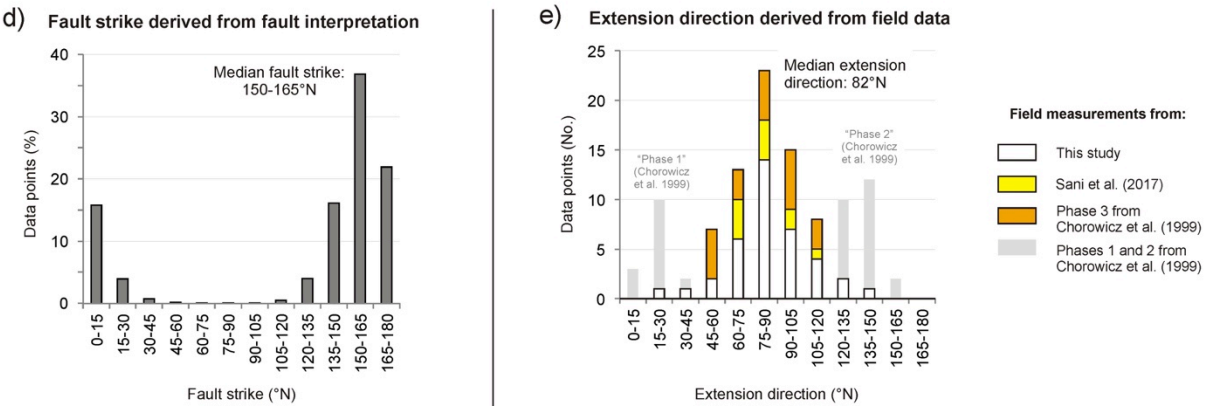
d)
Fault strike derived from fault interpretation
Median fault strike: 150-165°N
Data points (%)
Fault strike (°N)
0-15
15-30
30-45
45-60
60-75
75-90
90-105
105-120
120-135
135-150
150-165
165-180
e)
Extension direction derived from field data
Median extension direction: 82°N
"Phase 1" (Chorowicz et al. 1999)
"Phase 2" (Chorowicz et al. 1999)
Data points (No.)
Extension direction (°N)
Field measurements from:
This study
Sani et al. (2017)
Phase 3 from Chorowicz et al. (1999)
Phases 1 and 2 from Chorowicz et al. (1999)

Fig. 9. Overview of structural interpretation of the Western Afar Margin (WAM) as derived from DEM and satellite image analysis, as well as the assessment of novel and published field data. **(a)** WAM fault map as derived from satellite image and topography analysis. Interpreted faults are depicted with thin white lines, whereas thick white lines indicate recently active faults. **(b)** Combined fault kinematic analysis (data from Chorowicz et al. 1999; Sani et al. 2017 and new fieldwork) providing the extension directions of all points along the WAM. **(c)** Distribution of well-localized seismic events (of $\leq$ +-5 km in xyz directions) from our combined earthquake survey and recently active faults, as well as rift axes in Afar. Thick white lines indicate active faults/rift axes. Dotted lines indicate potential transverse structures (e.g. reactivated basement lineaments or rift linkage zones). Background topography is derived from ASTER data (90 m resolution). **(d)** Quantification of fault orientations along the WAM. **(e)** Quantification of extension directions derived from fault measurements.

5. Structural field data analysis

The original locations of fault measurements used for kinematic analysis, as well as the derived extension directions are presented in Figs. 5-7, of which a regional overview is provided in Fig. 9b, e. The underlying information (i.e. fault measurements, field photos and field book) is available in the supplementary materials (Zwaan et al. 2020c).

5.1. Regional kinematic interpretation

Kinematic analysis of our new field data yields an average extension direction between 75-90˚ N (Fig. 8e). However, we have (except for the fault at point ER1 affecting Quaternary deposits and the 1961 Karakore event, Figs. 5a, 7b-d) no specific age constraints on the fault planes on which our new kinematic measurements were taken, other than they mostly cut Trap basalts and follow the marginal trend. Yet, the mean extension direction is highly compatible with the results obtained by focal mechanism analysis (section 3.2, Fig. 4c, d, 9e). Furthermore, since the WAM is still actively deforming and the various faults we analyzed have likely experienced recent displacement (section 4.3), it is reasonable to infer that the calculated extension directions represent current tectonics. These results are subsequently complemented with kinematic data from faults affecting Quaternary deposits in Eritrea (Sani et al. (2017), and from the southern WAM (belonging to "phase 3", the youngest, currently active deformation stage reported by Chorowicz et al. 1999). By doing so, we obtain the first field-based overview of recent kinematics covering the whole length of the WAM (Fig 9b). Furthermore, the combined mean extension direction is the same as previously derived from focal mechanism analysis (i.e. 82˚N, section 3.2, Fig. 4c, d, 9e), underscoring the consistency of our interpretation.

Note that some faults in the Kobo and Borkenna areas provide deviating extension directions as well (Figs. 6b, 7b), which may simply be the result of local stress field changes that are not uncommon in nature (Roberts & Michetti 2004; Muirhead & Katterhorn 2018) and do not significantly change the outcomes of our analysis. Far to the south, we took fault measurements at two sites along the antithetic Karakore fault, among which a well-known outcrop containing slickensides that were probably exhumed during the events of 1961 (point 9.10, Fubelli &

Dramis 2011, Fig. 7b-c). These indicate pure normal faulting compatible with the shift of extension direction with respect to the northern parts of the WAM (Figs. 4c, d, 9b

5.2. Evidence of previous tectonic phases

Although the regional interpretation provide a clear overview of ongoing extension along the WAM, additional kinematic information on preceding tectonic phases was collected in the field. In the Abala area, we find evidence of ca. NNW-SSE extension recorded along ca. E-W striking normal faults oriented subparallel to the main faults of the Jurassic Mekele basin (Arkin et al. 1971; Beyth 1972; Amelu et al. 2018, Fig. 3a, point 1.1. in 5b) and are likely of the same age. Also a phase of NW-SE compression is recorded in Triassic units north of Abala (point 3.6, Fig. 5b), possibly related to Early Cretaceous tectonics (Bosellini et al. 2001). Finally, data from point 2.6. suggest a NNW-SSE extension (Fig. 5b), perhaps representing an early stage of Afar rifting (Chorowicz et al. 1999, see section 6.3).

6. Discussion

6.1. Synopsis of structural interpretation

Fault directions are dominantly NNW-SSE along most of the WAM (Figs. 9a, c), due to the en-echelon right-stepping arrangement of the margin and the associated marginal grabens that follow the same orientation (Fig. 9a, d). In the accommodation zones between the marginal grabens, faults do curve to a degree, but only south of ca. 10.5˚N, at the Arcuate Accomodation Zone does the prevailing fault trend truly deflect to align with the ca. SSW-NNE striking MER segments. The fault population is dominated by antithetic structures, a feature that is highly developed east of the marginal grabens between 10˚ and 12˚N, but less prevalent in the northern sectors of the WAM, possibly due to the difference in lithology (Figs. 3a, 5-7, 9a). Furthermore, in various places current fault activity occurs on or along the plateau, as well as along the antithetic faults (Fig. 9a). Also, earthquake and well data from the Abala and Kobo area, respectively, clearly indicate recent antithetic fault activity (Figs. 6c, d, 8), which fits very well with the concept of ongoing marginal flexure (Abbate et al. 1969; Kazmin et al. 1980; Wolfenden et al. 2005; Zwaan et al. 2020a). Well data also show marginal graben infill to be thin (< 250 m, Fig. 6c, d) and in spite of their impact on the landscape, marginal grabens and antithetic faults seem to form relatively small structures with respect to the large-scale (synthetic) escarpment faults that clearly must have accommodated large amounts of displacement over time.

6.2. Current tectonic regime in Afar

Large-scale earthquake analysis clearly shows that the whole of the WAM is still actively deforming and accounts for 1/3 of all seismic moment release. Subsequently, computing tectonic stress parameters from available focal mechanisms allows us to derive the current extension directions along the WAM, as well as in the adjacent Afar and the northernmost MER (Fig. 4c,

d). We find a general extension direction of 82˚N for the WAM, 66˚N for Afar and 108˚N for the MER, respectively (Fig. 4c, d).

Integrating our new fault measurements with published data from Chorowicz et al. (1999) and Sani et al. (2017) allows us to further assess the tectonic regime along the whole length of the WAM (Fig. 9b, e). Most faults have a normal fault character and indicate a ca. WSW-ENE extension direction (median: N82°E) that is highly compatible with the focal mechanism stress analysis.

We find that some data points deviate, but these are probably related to preceding tectonic phases (e.g. Jurassic opening of the Mekele basin and Early Cretaceous compression, Beyth 1972; Bosellini et al. 2001; Alemu et al. 2018, Fig. 5b) and potentially earlier phases of Afar rifting (Chorowicz et al. 1999) (see section 6.3), or may simply be the result of local stress field changes that are not uncommon in nature (e.g. Robers & Michetti 2004; Muirhead & Katterhorn 2018).

Combined with GPS motion from McClusky et al. (2010) and Saria et al. (2014) we can now construct a map of the current tectonics in the region (Fig. 10a). We find a curved pattern of extension directions from N82˚E along the WAM to N66˚E in Afar and ca. N48˚E at the Danakil Block. This is also inferred from seismic anisotropy, which shows a local rotation in the direction of maximum horizontal compression (SH_{Max}) (Illsley-Kemp et al., 2017). Furthermore, La Rosa et al. (2019) also record a ca. 60˚N extension along the Danakil axis. These reults are highly compatible with a rotational opening of Afar scenario due to the pivoting of the Danakil Block since ca. 11 Ma (e.g. Sichler 1980; Souriot & Brun 1992; Chorowicz et al. 1999; Collet et al. 2000; McClusky et al. 2010).

There is some evidence of non-rift parallel structures that transfer strain between laterally offset rifts as indicated the right-stepping zigzag pattern of earthquakes between the Danakil and Dabbahu rift axes (Figs. 4a, b, 8c). However, while these features are local complexities linking en-echelon and overlapping rift axes (e.g. Dumont et al. 2019; Pagli et al. 2019), they sit very much within a framework of anticlockwise rotation of the Danakil Block, as shown by GPS measurements and plate reconstructions (e.g. Collet et al. 2000; McClusky et al, 2010)

Finally in the MER to the south of the WAM, the average extension direction derived from earthquake focal mechanism analysis (N108˚E) is similar to that provided by GPS data (N96˚E, Saria et al. 2014, Fig. 10a), and Nubia-Somalia plate motion analysis (DeMets & Merkouriev 2016). This extension direction in combination with the orientation of the MER highlights the ongoing sinistral oblique extension there (e.g., Muluneh et al. 2014).

6.3. Past tectonic regime in Afar: the influence of Arabian plate rotation

By combining data from different sources, we show how the current tectonic regime of Afar is dominated by the rotation of the Danakil Block (Fig. 10a). However, rifting in Afar started between 25-31 Ma (Wolfenden et al. 2005; Ayele et al. 2007), much earlier than the rotation of this microplate initiated (ca. 11 Ma, McClusky et al. 2010). As pointed out by Smith (1993), the N-S orientation of the WAM in combination with the counterclockwise rotation of the Arabian plate about a pole near Egypt (McKenzie et al. 1970; ArRajehi et al. 2010) demands a local sinistral oblique extension along the margin (Fig. 10b), which is comparable to the initial “NE-SW” extension direction reported by Chorowicz et al. (1999, Fig. 11b). Such an extension

direction along the N-S margin could also elegantly explain the remarkable right-stepping en echelon arrangement of the WAM, which is typical for oblique rifting and can easily reactivate during multiphase rifting, controlling the locus of subsequent faulting (e.g. Keep & McClay 1997; Bonini et al. 1997). Similar geometrical relations also explain the oblique fault structures observed in the Gulf of Suez, as well as those along the margins and spreading ridge of the Gulf of Aden (Smith 1993, Leroy 2012 and references therein, Figs. 1a, 10b). The fact that we currently observe an almost E-W extension along the WAM thus indicates a significant local tectonic anomaly, which we can only attribute to the rotational opening of Afar (Kogan et al. 2012).

We therefore propose the following tectonic history of the WAM (Fig. 10c-f). Sinistral oblique extension occurred at the start of Afar rifting as the Arabian plate started rotating, and rifting propagated from the Gulf of Aden in the east to the Red Sea in the west (Figs. 1, 10c, d). We note that Bosworth et al. (2005) and Bosworth (2015) describe slight variations in extension direction, but these are minor changes and would always cause sinistral oblique extension along the WAM, so that our pure rotational model remains valid for a large-scale interpretation. The N-S orientation of the WAM was either controlled by the reactivation of Panafrican lineaments (Drury et al. 1994; Chorowicz et al. 1999; Ghebreab & Talbot 2000; Collet et al. 2000) or by the northward extension of the weak lithospheric mantle below Afar forming a distinct rheological contrast (Chang et al., 2011; Hansen & Nyblade, 2013; Molnar et al. 2017). Initial rifting was distributed (e.g. Stab et al. 2016), leading to a wide rift zone with the later Danakil Block as a part of the extending terrain (Morton and Black 1975; Collet et al. 2000; Redfield et al. 2003, Fig. 10d). Subsequently, two rift axes (the Red Sea and Danakil axes) formed on both sides of the Danakil Block (Fig. 10e). This overlapping rift arrangement caused a modification of the regional tectonic setting and the rotation of the Danakil Block from ca. 11 Ma on (Eagles et al. 2002; McClusky et al. 2010; Reilinger & McClusky 2011; Kogan et al. 2012; Molnar et al. 2017). As a result, the local stress field along the WAM is now almost E-W (Figs. 4c, 9b, e, 10a). Around the same time (11 Ma) also the MER became part of the Afar triple junction (Wolfenden et al. 2004, Fig. 10e). Based on field data, Chorowicz et al. (1999) propose that the localization of the MER was preceded by a short phase of widespread NW-SE extension. Yet many other studies suggest that extension directions in the MER were always similar to the near E-W extension currently constrained by means of GPS surveys and focal mechanisms, a view we adopted in our reconstruction (Saria et al. 2014, DeMets & Merkouriev 2016 and references therein, Figs. 4c, 10a, d, e).

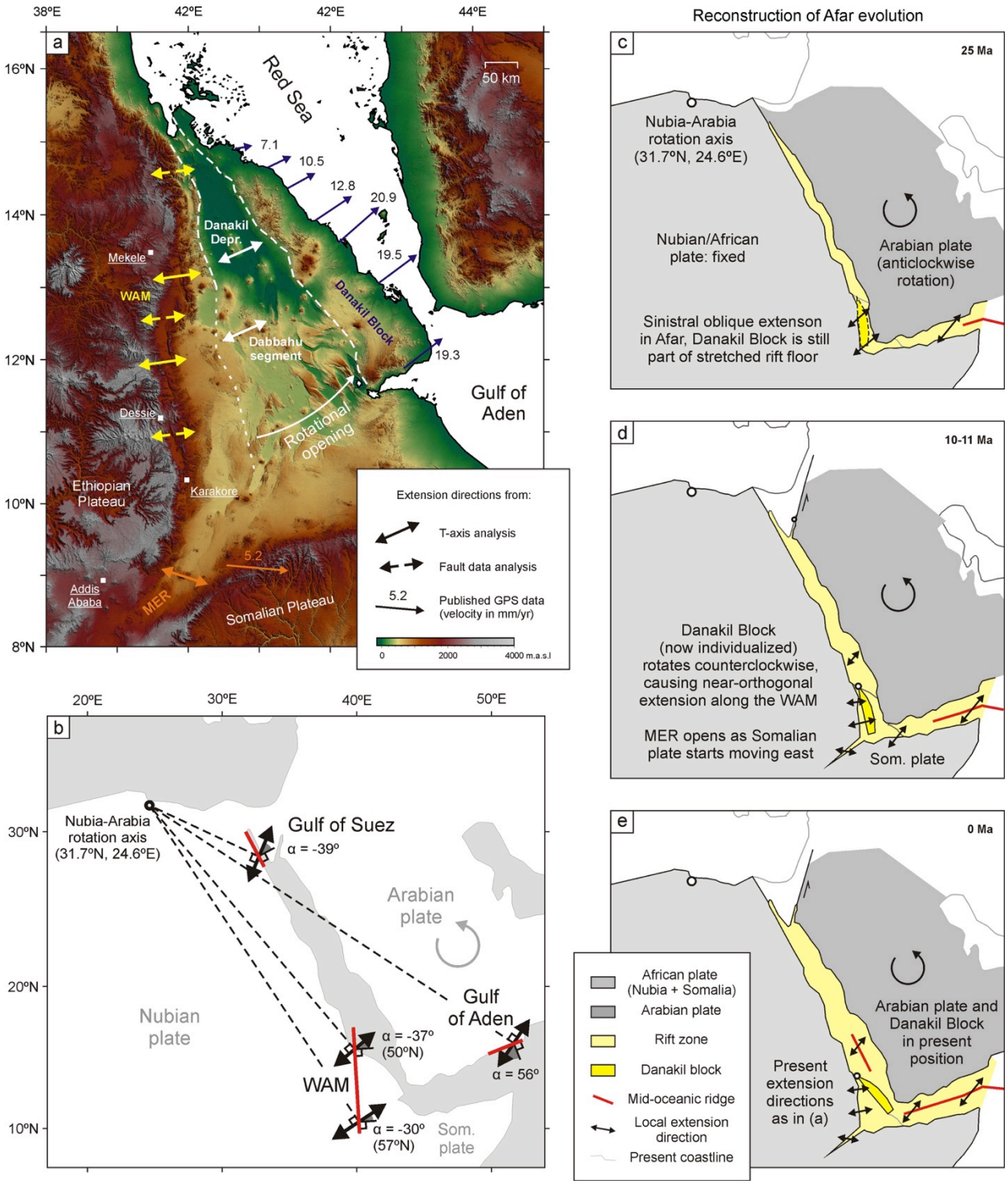

Fig. 10. Interpretation of regional tectonics. **(a)** Combined overview of current tectonic setting in Afar as derived from (1) Focal mechanism analysis, (2) field measurements (based on data from Chorowicz et al. 1999; Sani et al. 2017 and this study) and (3) GPS data (McClusky et al. 2010 and Saria et al. 2014). MER: Main Ethiopian Rift. **(b)** Theoretical extension directions (described by angle α between the normal to the rift trend and the general extension direction) in the Red Sea, Gulf of Aden and along the Western Afar Margin (WAM) as a result of the rotation of the

Arabian plate about a pole at 31.7˚N, 24.6˚E (ArRajehi et al. 2010). The ca. N-S orientation of the WAM should result in a ca. NE-SW extension direction (50˚-57˚N) there, similar to the first (sinistral) extension phase described by Chorowicz et al. (1999). Modified after Smith (1993). **(c-e)** Proposed multiphase evolution of Afar within the regional tectonic framework and effects on extension directions along the WAM. Initial sinistral oblique extension due to the rotation of the Arabian plate (c) is followed by a near-orthogonal extension due to the individual motion of the Danakil block (d-e). Based on Smith (1993), Bosworth et al. (2005), ArRajehi et al. (2010) and Bosworth (2015).

6.4. Regional and global significance

In the above paragraph we describe the structural features of the WAM and how Afar and its western margin have experienced two phases of rotational extension, the first related to the motion of the Arabian plate and the second related to the opening of the Danakil Depression.

As discussed in the review by Zwaan et al. (2020a) various contrasting scenarios have been proposed to explain the current structural architecture of the WAM, most of which are based on a small area of the WAM and extrapolated over the whole margin. We hope that the data presented in this work will serve as a basis to better constrain the structural evolution of the margin as a whole. Our new data confirms the presence of active antithetic faulting and shallow underfilled marginal grabens, hinting towards recent marginal flexure (e.g. Abbate & Sagri 1969; Wolfenden et al. 2005; Illsley-Kemp et al. 2018a), as well as the influence of multiphase (rotational/oblique) extension and fault reactivation during rifting. Both these factors need to be considered for any complete model.

Afar is often seen as a key location to study continental break-up and passive margin formation in magma-rich environments. Our constraints on extension direction in Afar from fault slip and focal mechanism data shows significant rotation of extension over relatively short length scales, best explained by rotational tectonics. This provides further support to the growing body of evidence that plate rotation needs to be considered when interpreting timing of rift initiation, as well as spatial and temporal variations in extension amount and direction (e.g. Molnar et al. 2017, 2018; Mondy et al. 2018; Zwaan et al. 2020b). For example, the large-scale rotation of the Arabian plate as well as associated extension gradients (both in rate and amount of extension) can be found along passive margins worldwide, and various passive margins have experienced changes in extension direction during their evolution (e.g. the NE Atlantic; Gaina et al. 2009; Brune et al. 2018). Furthermore, the ongoing tectonic activity of the WAM after the formation of the magmatic segments in Afar suggests that seafloor spreading is not fully established in Afar. In addition, pervasive antithetic faulting has been observed along various magma-rich passive margins (e.g. the South Atlantic margins, Paton et al. 2017; Norcliffe et al. 2018) and it appears that marginal graben-like structures are in fact present along the Uruguayan margin (Tugend et al. 2018). We conclude that the WAM provides highly valuable insights concerning (magma-rich) passive margin development.

7. Conclusion

In this paper, we have combined seismicity analysis, large-scale structural interpretation, new and published (field) data and well logs to create an up to date description of the structural framework of the Western Afar Margin (WAM) in East Africa and the associated tectonic implications. We find that:

- Although Afar is in the final stages of continental break-up and extension has largely shifted from the WAM to central Afar, earthquake and seismic moment release (SMR) data show that significant deformation is still taking place along the whole of the WAM, which is clearly not a "true" passive margin yet.

- Tectonic stress parameters derived from focal mechanism analysis reveal different extension directions along the WAM (82˚N), Afar (66˚N) and in the Main Ethiopian Rift (108˚N). Analysis of new and published fault measurements also reveals an extension direction of 82˚N along the WAM.

- The N-S oriented WAM forms a major transition between the Ethiopian Plateau and Afar, and is characterized by NNW-SSE normal faulting, a significant part of these antithetic in nature, and an associated series en echelon marginal grabens.

- Geomorphology and detailed earthquake analysis suggests that the antithetic faults are currently accommodating significant deformation along the margin. Yet we also find evidence of active deformation at of the Ethiopian Plateau and recognize that the large escarpment faults must have accommodated large amounts of slip over time.

- We present the first-ever borehole-calibrated sections of the WAM, which highlight the limited sedimentary infill of the marginal grabens and support the interpretation that the antithetic faults are currently accommodating significant deformation along the WAM.

- Fault kinematic analysis on new fault measurements complemented by published fault data allows us to create the first fault kinematic analysis of the WAM, indicating a current 82˚N extension direction, highly compatible with the results from focal mechanism analysis.

- By combining the results of fault kinematic analysis, tectonic stress estimations and published GPS data we create a integrated overview of active deformation in Afar, which provides strong evidence that current tectonics in Afar are dominated by the rotation of the Danakil Block, and to a lesser degree the opening of the Main Ethiopian Rift.

- The earlier stages of Afar development (25-11 Ma) were however most likely directly related to the rotation of the Arabian plate and the N-S orientation of the future WAM, the latter possibly as a result of reactivated Pan-African lineaments, and involved sinistral oblique extension creating the characteristic en echelon fault arrangement of the margin. Only after the Danakil started its rotation around 11 Ma, the current tectonic regime was emplaced and the en echelon faults reactivated under near-EW extension.

- Any complete scenario to explain the structural evolution of the WAM should take into account, among other factors, the multi-phase tectonic history of the WAM, the syntethic escarpment and marginal graben development, as well as the current antithetic fault activity we observe.

- The findings of this study are not only relevant for a better understanding of the WAM, but also for the understanding of the role of (multiphase) oblique and rotational extension during rifting and (magma-rich) passive margin evolution in general.

Acknowledgments

We would like to thank Tim Greenfield and Emma Chambers for their help with GMT. Said Abdu (Water Resource Mine and Energy office of Tigray, Alamata), Fanuel Sharew, Abrha Shumey and Berhe Abrha (Water Resource Mine and Energy office of Raya Azebo, Mahoni), Solomon Arbsie (Kobo Girana Valley Development Program, Kobo) and Belay Amberber (Woldia University, Woldiya) are gratefully acknowledged for their help in the field and for providing well logs. We would like to especially express our gratitude to Solomon Belay Gebreegziabher (Etioder, Addis Ababa) for patiently driving us to every outcrop we fancied. Carolina Pagli, Valentin Rime and Marco Benvenuti helped us to collect the earthquake datasets and maps of the study area. Fault data analysis was done using Win-Tensor, a software developed by Dr. Damien Delvaux, Royal Museum for Central Africa, Tervuren, Belgium. We thank two anonymous reviewers for their constructive feedback that greatly helped to improve the final work. Kirsten Elger and Matthias Rosenau kindly assisted us to publish the supplementary materials to this paper in the form of an Open Access GFZ Data Publication (Zwaan et al. 2020c, http://doi.org/10.5880/fidgeo.2020.017).

This project was funded by the Swiss National Science Foundation (Early Postdoc Mobility grant P2BEP2_178523, http://p3.snf.ch/Project-178523) awarded to FZ. FS received financial support from the Ministero Università e Ricerca (grant MiUR-FFABR2017) and the Università degli Studi di Firenze (grant 2018). PRIN grant 2017P9AT72 covered publication costs. FIK is supported by the ECLIPSE program, funded by the New Zealand Ministry of Business Innovation and Employment.

Data availability

Extensive supplementary material is publicly available in the form of a GFZ Data Publication (Zwaan et al. 2020c): http://doi.org/10.5880/fidgeo.2020.017.

References

Abbate, E., Sagri, M., 1969. Dati e considerazioni sul margine orientale dell'altiplano etiopico nelle province del Tigrai e del Wollo. Boll Soc Geol It 88, 489–497. NO DOI

Abbate, E., Woldehaimanot, B., Bruni, P., Falorni, P., Papini, M., Sagri, M., Girmat, S., Tecle, T.M., 2004. Geology of the Homo-bearing Pleistocene Dandiero Basin (Buia Region, Eritrean Danakil Depression). Rivista Italiana di Paleontologia e Stratigrafia 110, 5-34. https://doi.org/10.13130/2039-4942/5761

Abbate, E., Bruni, P., Sagri, M., 2015. Geology of Ethiopia: A Review and Geomorphological Perspectives. In: Billi, P. (ed.) Landscapes and Landforms of Ethiopia, World Geomorphological Landscapes. Springer Science+Business Media, Dordrecht, 33-64. https://doi.org/10.1007/978-94-017-8026-1_2

Alemu, T., Abdelsalam, M.G., Dawit, E.L., Atnafu, B., Mickus, K.L., 2018. The Paleozoic e Mesozoic Mekele Sedimentary Basin in Ethiopia: An example of an exhumed IntraCONtinental Sag (ICONS) basin. Journal of African Earth Sciences 143, 40-58. https://doi.org/10.1016/j.jafrearsci.2018.03.010

Argent, J.D., Stewart, S.A., Underhill, J.R., 2000. Controls on the Lower Cretaceous Punt Sandstone Mem- ber, a massive deep-water clastic deposystem, Inner Moray Firth, UK North Sea. Petroleum Geoscience, 6, 275–285 https://doi.org/10.1144/petgeo.6.3.275

Arkin, Y., Beyth, M., Dow, D.B., Levitte, D., Temesgen, H., Tsegaye, H., 1971. Geological map of Mekele sheet area Sheet ND 37–11, Tigre province. Imperial Ethiopian Government, Ministry of Mines, Geological Survey of Ethiopia, Addis Ababa.

Arnold, R., Townend, J., 2007. A Bayesian approach to estimating tectonic stress from seismological data. Geophysical Journal International 170, 1336-1356. https://doi.org/10.1111/j.1365-246X.2007.03485.x

ArRajehi, A., McCluskey, S., Reilinger, R., Daoud, M., Alchalbi, A., Egintav, S., Gomez, F., Sholan, J., Bou-Rabee, F., Ogubazghi, G., Haileab, B., Fisseha, S., Asfaw, L., Mahmoud, S., Rayan, A., Bendik. R., Kogan, L., 2010. Geodetic constraints on present-day motion of the Arabian Plate: Implications for Red Sea and Gulf of Aden rifting. Tectonics, 29, TC3011. https://doi.org/10.1029/2009TC002482

Augustin, N., Devey, C.W., Van der Zwan, F.M., Feldens, P., Tominaga, M., Bantan, R.A., Kwasnitschka, T., 2014. The rifting to spreading transition in the Red Sea. Earth and Planetary Science Letters 395, 217-230. https://doi.org/10.1016/j.epsl.2014.03.047

Ayele, A., Stuart, G., Bastow I., Keir, D., 2007. The August 2002 earthquake sequence in north Afar: Insights into the neotectonics of the Danakil microplate. Journal of African Earth Sciences 48, 70-79. https://doi.org/10.1016/j.jafrearsci.2006.06.011

Ayalew, D., Ebinger, C., Bourdon, E., Wolfenden, E., Yirgu, G., Grassineau, N., 2006. Temporal compositional variation of syn-rift rhyolites along the western margin of the southern Red Sea and northern Main Ethiopian Rift. In: Yirgu, G., Ebinger, C.J., Maguire, P.K.H. (eds) 2006. The

858 Afar Volcanic Province within the East African Rift System. Geological Society, London,
859 Special Publications, 259, 121-130. https://doi.org/10.1144/GSL.SP.2006.259.01.10

860 Baker, B.H., Mohr, P.A., Williams, L.A.J., 1972. Geology of the Eastern Rift System of Africa.
861 GSA Special Paper 136. https://doi.org/10.1130/SPE136

862 Barberi, F., Borsi, S., Ferrara, G. Marinelli, G., Varet, J., 1970. Relations between Tectonics and
863 Magmatology in the Northern Danakil Depression (Ethiopia). Philosophical Transactions of The
864 Royal Society A: Mathematical, Physical and Engineering Sciences 267. 293-311.
865 https://doi.org/10.1098/rsta.1970.0037

866 Barberi, F., Giglia, G., Marinelli. G., Santecroce, R., Tazieff, H., Varet, J. Bonatti, E., Borsi, S.,
867 Cheminiée, J.L., Faure, H., Ferrara, G., Marini, M., 1972. Geological Map of the Danakil
868 Depression. Société GÉOTECHNIP 78, la Celle-Saint Cloud, France.

869 Barberi, F., Varet, J., 1977. Volcanism of Afar: Small-scale plate tectonics implications. GSA
870 Bulletin 88, 1251-1266. https://doi.org/10.1130/0016-7606(1977)88<1251:VOASPT>2.0.CO;2

871 Barberi, F., Santacroce, R., 1980. The Afar Stratoid Series and the magmatic evolution of East
872 African rift system. Bulletin de la Société Géologique de France S7-XXII, 891-899.
873 https://doi.org/10.2113/gssgfbull.S7-XXII.6.891

874 Barnie, T.D., Keir, D., Hamling, I., Hofmann, B., Belachew, M., Carn, S., Eastwell, D.,
875 Hammond, J.O.S., Ayele, A., Oppenheimer, C., Wright, T., 2016. A multidisciplinary study of
876 the final episode of the Manda Hararo dyke sequence, Ethiopia, and implications for trends in
877 volcanism during the rifting cycle. In: Wright, T.J., Ayele, A, Ferguson, D.J., Kidane, T., Vye-
878 Brown, C. (eds.) Magmatic Rifting and Active Volcanism. Geological Socitey of London Special
879 Publication 420, 149-163. https://doi.org/10.1144/SP420.6

880 Belachew, M., Ebinger, C., Coté, D., Keir, D., Rowland, J. V., Hammond, J.O.S., Ayele, A.,
881 2011. Comparison of dike intrusions in an incipient seafloor-spreading segment in Afar,
882 Ethiopia: Seismicity perspectives. Journal of Geophysical Research, 116(B6), B06405.
883 https://doi.org/10.1029/2010JB007908

884 Bellahsen., N., Facenna C., Funiciello, F., Daniel, J.M., Jolivet, L., 2003. Why did Arabia
885 separate from Africa? Insights from 3-D laboratory experiments. Earth and Planetary Science
886 Letters 216, 365-381. https://doi.org/10.1016/S0012-821X(03)00516-8

887 Berhe, S.M., 1985. Geological map of Dire Dawa (Sheet NC37–12). Ethiopian Institute of
888 Geological Surveys, Addis Ababa.

889 Berhe, S.M., 1986. Geologic and geochronologic constraints on the evolution of the Red Sea–
890 Gulf of Aden and Afar Depression. Journal of African Earth Sciences 5, 101–117.
891 https://doi.org/10.1016/0899-5362(86)90001-1

892 Beyene, A., Abdelsalam, M.G., 2005. Tectonics of the Afar Depression: A review and synthesis.
893 Journal of African Earth Sciences, 41, 41-59. https://doi.org/10.1016/j.jafrearsci.2005.03.003

Beyth, M., 1972. Paleozoic-Mesozoic Sedimentary Basin of Mekele Outlier, Northern Ethiopia. AAPG Bulletin 56, 2426-2439. https://doi.org/10.1306/819A422A-16C5-11D7-8645000102C1865D

Billi, P., 2015. Geomorphology of Ephemeral Streams in the Kobo Basin. In: Billi, P. (ed) Landscapes and Landformes of Ethiopia. Springer Science and Business Media Dordrecht. https://doi.org/10.1007/978-94-017-8026-1_12

Bosellini, A., Russo, A., Assefa, G., 2001. The Mesozoic succession of Dire Dawa, Harar Province, Ethiopia. Journal of African Earth Sciences 32, 403-417. https://doi.org/10.1016/S0899-5362(01)90105-8

Bosworth. W., Huchon P., McClay, K., 2005. The Red Sea and Gulf of Aden Basins. Journal of African Earth Sciences 43, 334-378. https://doi.org/10.1016/j.jafrearsci.2005.07.020

Bosworth, W., 2015. Geological evolution of the Red Sea: Historical background, review, and synthesis. In: Rasul N., Stewart I. (eds) The Red Sea. Springer Earth System Sciences. Springer, Berlin, Heidelberg. https://doi.org/10.1007/978-3-662-45201-1_3

Brune, S., 2016. Rifts and rifted margins: A review of geodynamic processes and natural hazards, from J.C. Duarte, W. P. Schellart (Eds.) Plate Boundaries and Natural Hazards. AGU Geophysical Monograph 219. https://doi.org/10.1002/9781119054146.ch2

Brune, S., Williams, S.E., Müller, R.D., 2018. Oblique rifting: the rule, not the exception, Solid Earth, 9, 1187–1206. https://doi.org/10.5194/se-9-1187-2018

Catuneanu, O., Abreu, V., Bhattacharya, J.P., Blum, M.D., Dalrymple, R.W., Eriksson, P.G., Fielding, C.R., Fisher, W.L., Galloway, W.E., Gibling, M.R., Giles, K.A., Holbrook, J.M., Jordan, R., Kendall, C.G.St.C., Macurda, B., Martinsen, O.J., Miall, A.D., Neal, J.E., Nummedal, D., Pomar, L., Posamentier, H.W., Pratt, B.R., Sarg, J.F., Shanley, K.W., Steel, R.J., Strasser, A., Tucker, M.E., Winker, C., 2009. Towards the standardization of sequence stratigraphy. Earth-Science Reviews 92, 1-33. https://doi.org/10.1016/j.earscirev.2008.10.003

Chang, S-J., Merino, M., Van der Lee, S., Stein, S., Stein, C.A., 2011. Mantle flow beneath Arabia offset from the opening Red Sea. Geophysical Research Letters 38, L04301. https://doi.org/10.1029/2010GL045852

Chorowicz, J., Collet, B., Bonavia, F., Korme, T., 1999. Left-lateral strike-slip tectonics and gravity induced individualisation of wide continental blocks in the western Afar margin. Eclogae Geologicae Helvetiae, 92, 149-158. http://doi.org/10.5169/seals-168656

Cochran, J.R., 2005. Northern Red Sea: nucleation of an oceanic spreading cen- ter within a continental rift. Geochemistry, Geophysics, Geosystems 6, Q03006. http://dx.doi.org/10.1029/2004GC000826

Collet, B., Taud, H., Parrot, J.F., Bonavia, F., Chorowicz, J., 2000. A new kinematic approach for the Danakil block using a Digital Elevation Model representation. Tectonophysics 316, 343-357. https://doi.org/10.1016/S0040-1951(99)00263-2

931 Coltorti, M., Dramis, F., Ollier, C.D., 2007. Planation surfaces in Northern Ethiopia.
932 Geomorphology 89, 287–296. https://doi.org/10.1016/j.geomorph.2006.12.007

933 Coltorti, M., Firuzabadi, D., Borri, A., Fantozzi, P., Pieruccini, P., 2015. Planation Surfaces and
934 the Long-term Geomorphological Evolution of Ethiopia. In: Billi, P. (ed) Landscapes and
935 Landformes of Ethiopia. Springer Science and Business Media Dordrecht.
936 https://doi.org/10.1007/978-94-017-8026-1_5

937 Corti, G., Bastow, I.D., Keir, D., Pagli, C., Baker, E., 2015. Rift-Related Morphology of the Afar
938 Depression. In: Billi, P. (ed.) Landscapes and Landforms of Ethiopia, World Geomorphological
939 Landscapes. Springer Science and Business Media, Dordrecht, 251-274.
940 https://doi.org/10.1007/978-94-017-8026-1_15

941 CMT (Global Centroid-Moment-Tensor) Project. https://www.globalcmt.org

942 D'Acremont, E., Leroy, S., Maia, M., Patriat, P., Berslier, M.O., Bellahsen, N., Fournier, M.,
943 Gente, P., 2006. Structure and evolution of the eastern Gulf of Aden: Insights from magnetic and
944 gravity data. Geophysical Journal International 165, 786–803. https://doi.org/10.1111/j.1365

945 d'Acremont, E., Leroy, S., Maia, M., Gente, P., Autin, J., 2010. Volcanism, jump and
946 propagation on the Sheba ridge, eastern Gulf of Aden: segmentation evolution and implications
947 for oceanic accretion processes. Geophysical Journal International 180 (2), 535–551.
948 http://dx.doi.org/10.1111/j.1365-1246X.2009.04448.x

949 Davison, I., Underhill, J.R., 2012. Tectonics and sedimentation in extensional rifts: Implications
950 for petroleum systems. In: Gao, D. (ed). Tectonics and sedimentation: Implications for petroleum
951 systems. AAPG Memoir 100, 15–42. https://doi.org/10.1306/13351547M1001556

952 Davison, I., Al-Kadasi, M., Al-Khirbash, S., Al-Subbary, A.K., Baker, J., Blakey, S., Bosence,
953 D., Dart, C., Heaton, R., McClay, K., Menzies, M., Nichols, G., Owen, L., Yelland, A., 1994.
954 Geological evolution of the southeastern Red Sea Rift margin, Republic of Yemen. Geological
955 Society of America Bulletin 106, 1474–1493. https://doi.org/10.1130/0016-
956 7606(1994)106<1474:GEOTSR>2.3.CO;2

957 Davison, I., Tatnell, M.R., Owen, L.A., Jenkins, G., Baker, J., 1998. Tectonic geomorphology
958 and rates of crustal processes along the Red Sea margin, north-west Yemen. In: Purser, B.H.,
959 Bosence, D.W.J. (Eds.), Sedimentation and Tectonics in Rift Basins: Red Sea–Gulf of Aden.
960 Chapman and Hall, London, 595–612. https://doi.org/10.1007/978-94-011-4930-3_32

961 Delvaux, D., Sperner, B., 2003. Stress tensor inversion from fault kinematic indicators and focal
962 mechanism data: the TENSOR program. In: Nieuwland, D. (ed) New Insights into Structural
963 Interpretation and Modelling. Geological Society, London, Special Publications, 212: 75-100.
964 https://doi.org/10.1144/GSL.SP.2003.212.01.06

965 DeMets C., Merkouriev, S., 2016. High-resolution estimates of Nubia–Somalia plate motion
966 since 20 Ma from reconstructions of the Southwest Indian Ridge, Red Sea and Gulf of Aden.
967 Geophysical Journal International 207, 317–332. https://doi.org/10.1093/gji/ggw276

968 Dumont, S., Klinger, Y., Socquet, A., Escartín, J., Grandin, R., Jacques, E., Medynski, S.,
969 Doubre, S., 2019. Rifting processes at a continent-ocean transition rift revealed by fault analysis.
970 Example of Dabbahu- Manda-Hararo rift (Ethiopia). Tectonics, 38, 190–214. https://doi.org/
971 10.1029/2018TC005141

972 Drury, S.A., Kelley, S.P., Berhe, S.M., Collier, R.E.Ll., Abraha, M., 1994. Structures related to
973 Red Sea evolution in northern Eritrea. Tectonics 13, 1371-1380.
974 https://doi.org/10.1029/94TC01990

975 Dziewonski, A.M., Chou, T.-A., Woodhouse, J.H., 1981. Determination of earthquake source
976 parameters from waveform data for studies of global and regional seismicity. Journal of
977 Geophysical Research 86, 2825-2852. https://doi.org/10.1029/JB086iB04p02825

978 Eagles, G., Gloaguen, R., Ebinger, C., 2002. Kinematics of the Danakil microplate. Earth and
979 Planetary Science Letters 203, 607-620. https://doi.org/10.1016/S0012-821X(02)00916-0

980 Ebinger, C.J., Keir, D., Ayele, A., Calais, E., Wrigth, T.J., Belachew, M., Belachew, M.,
981 Hammond, J.O.S., Campbell, E., Buck, W.R. 2008. Capturing magma intrusion and faulting
982 processes during continental rupture: seismicity of the Dabbahu (Afar) rift. Geophysical Journal
983 International 174, 1138-1152. https://doi.org/10.1111/j.1365-246X.2008.03877.x

984 Ekström, G., Nettles, M., Dziewonski, A.M., 2012. The global CMT project 2004-2010:
985 Centroid-moment tensors for 13,017 earthquakes. Physics of the Earth and Planetary Interiors
986 200-201, 1-9. https://doi.org/10.1016/j.pepi.2012.04.002

987 Fazzini, M., Bisci, C., Billi, P. 2015. The Climate of Ethiopia. In: Billi, P. (ed) Landscapes and
988 Landformes of Ethiopia. Springer Science and Business Media Dordrecht.
989 https://doi.org/10.1007/978-94-017-8026-1_3

990 Fournier, M., Chamot-Rooke, N., Petit, C., Huchon, P., Al-Kathiri, A., Audin, L., Beslier, M.-O.,
991 d'Acremont, E., Fabbri, O., Fleury, J.-M., Khanbari, K., Lepvrier, C., Leroy, S., Maillot, B.,
992 Merkouriev, S., 2010. Arabia–Somalia plate kinematics, evolution of the Aden–Owen–Carlsberg
993 triple junction, and opening of the Gulf of Aden. Journal of Geophysical Research 115.
994 http://dx.doi.org/10.1029/2008jb006257

995 Fubelli, G., Abebe, B., Drabis, F., Vinci. S., 2008. Geomorphological evolution and present-day
996 processes in the Dessie Graben (Wollo, Ethiopia). Catena 75, 28-37.
997 https://doi.org/10.1016/j.catena.2008.04.001

998 Fubelli G, Dramis F., 2011. Coseismic surface faulting in the Kara Kore area (Wollo) caused by
999 the May 29, 1961 Earthquake. In: Nyssen, Asrat, A., Dramis, F., Umer, M. (eds) Pre-conference
1000 excursion guide: tectonic landforms and volcanism in the Southern Afar. IAG regional
1001 conference 2011 geomorphology for human adaptation to changing tropical environments, Addis
1002 Ababa, Ethiopia, 18–22 Feb 2011, 5-7.

1003 Fubelli, G., Dramis, F., 2015. Geo-hazards in Ethiopia. In: Billi, P. (ed) Landscapes and
1004 Landformes of Ethiopia. Springer Science and Business Media Dordrecht.
1005 https://doi.org/10.1007/978-94-017-8026-1_20

1006 Gaina, C., Gernigon, L., Ball. P., 2009. Palaeocene–Recent plate boundaries in the NE Atlantic
1007 and the formation of the Jan Mayen microcontinent. Journal of the Geological Society, London
1008 166, 601-616. https://doi.org/10.1144/0016-76492008-112

1009 Gani, N.D.S., Gani, M.R., Abdelsalam, M.G., 2007. Blue Nile incision on the Ethiopian Plateau:
1010 Pulsed plateau growth, Pliocene uplift, and hominin evolution. GSA Today 17.
1011 https://doi.org/10.1130/GSAT01709A.1

1012 Garland, C.B., 1980. Geology of the Adigrat Area. Provisional Military Govt. of Socialist
1013 Ethiopia, Ministry of Mines, Energy & Water Resources, Geological Survey of Ethiopia.

1014 Geoffroy, L., Huchon, P., Khanbari, K., 1998. Did Yemeni tertiary granites intrude neck zones of
1015 a stretched continental upper crust? Terra Nova 10, 196–200. https://doi.org/10.1046/j.1365-
1016 3121.1998.00194.x

1017 Ghebreab, W., Talbot, C.J., 2000. Red Sea extension influenced by Pan-African tectonic grain in
1018 eastern Eritrea. Journal of Structural Geology 22, 931-946. https://doi.org/10.1016/S0191-
1019 8141(00)00022-5

1020 Gouin, P., 1970. A discussion on the structure and evolution of the Red Sea and the nature of the
1021 Red Sea, Gulf of Aden and Ethiopia rift junction - Seismic and gravity data from Afar in relation
1022 to surrounding areas. Philosophical Transactions of the Royal Society of London. Series A,
1023 Mathematical and Physical Sciences 267, 339-358. http://doi.org/10.1098/rsta.1970.0040

1024 Gouin, P., 1979. Earthquake history of Ethiopia and the Horn of Africa. International
1025 Development Research Centre, Ottawa.

1026 Hagos, M., Konko, B., Ahmed, J., 2016. A preliminary geological and generalized stratigraphy
1027 of Western Margin of Northern Afar Depression, Dallol area, Northern Ethiopia. Momona
1028 Ethiopian Journal of Science 8, 1-22. http://dx.doi.org/10.4314/mejs.v8i1.1

1029 Hammond, J.O.S., Kendall, J.-M., Stuart, G.W., Keir, D., Ebinger, C., Ayele, A., Belachew, M.,
1030 2011. The nature of the crust beneath the Afar triple junction: Evidence from receiver functions.
1031 Geochemistry, Geophysics, Geosystems, 12, Q12004. https://doi.org/10.1029/2011GC003738

1032 Hansen, S., Nyblade, A.A., 2013. The deep seismic structure of the Ethiopia/Afar hotspot and the
1033 African superplume. Geophysical Journal International 194, 118-124.
1034 https://doi.org/10.1093/gji/ggt116

1035 Haq, B.U., Hardenbol, J., Vail, P.R., 1987. Chronology of Fluctuating Sea Levels Since the
1036 Triassic. Science 235, 1156-1167. https://doi.org/10.1126/science.235.4793.1156

1037 Hayward, N.J., Ebinger, C.J., 1996. Variations in the along-axis segmentation of the Afar Rift
1038 system. Tectonics 15, 244-257. https://doi.org/10.1029/95TC02292

1039 Hoffmann, C., Courtillot, V., Féraud, G., Rochetter, P., Yirgu, G., Ketefo, E., Pik, R., 1997.
1040 Timing of the Ethiopian flood basalt event and implications for plume birth and global change.
1041 Nature 389, 838-841. https://doi.org/10.1038/39853

1042 Hofstetter, R., Beyth, N., 2003. The Afar Depression: interpretation of the 1960–2000
1043 earthquakes. Geophysical Journal International 155, 715-732. https://doi.org/10.1046/j.1365-
1044 246X.2003.02080.x

1045 Illsley-Kemp, F., Savage, M.K., Keir, D., Hirschberg, H.P., Bull, J.M., Gernon, T.M.,
1046 Hammond, J.O., Kendall, J.M., Ayele, A. Goitom, B., 2017. Extension and stress during
1047 continental breakup: Seismic anisotropy of the crust in Northern Afar. Earth and Planetary
1048 Science Letters 477, 41-51. https://doi.org/10.1016/j.epsl.2017.08.014

1049 Illsley-Kemp, F., Keir, D., Bull, J.M., Gernon, T.M., Ebinger, C., Ayele, A., Hammond, J.O.S.,
1050 Kendall, J.-M., Goitom, B., Belachew, M., 2018a. Seismicity during continental breakup in the
1051 Red Sea rift of Northern Afar. Journal of Geophysical Research: Solid Earth, 123.
1052 https://doi.org/10.1002/2017JB014902

1053 Illsley-Kemp, F., Bull, J.M., Keir, D., Gerya, T., Pagli, C., Gernon, T., Ayele, A., Goitom, B.,
1054 Hammond, J.O.S., Kendall, J.M., 2018b. Initiation of a proto-transform fault prior to seafloor
1055 spreading. Geochemistry, Geophysics, Geosystems 19, 4744–4756.
1056 https://doi.org/10.1029/2018GC007947

1057 Izzeldin, A.Y., 1987. Seismic, gravity and magnetic surveys in the central part of the Red-Sea –
1058 their interpretation and implications for the structure and evolution of the Red-Sea.
1059 Tectonophysics 143, 269–306. https://doi.org/10.1016/0040-1951(87)90214-9

1060 Kazmin, V., 1972. Geological map of Ethiopia. Geological Survey of Ethiopia, Ministry of
1061 Mines, Energy and Water Resources, Addis Ababa.
1062 https://esdac.jrc.ec.europa.eu/images/Eudasm/Africa/images/maps/download/afr_etgm.jpg

1063 Kazmin, V., Garland, C.R., Aklilu, A., Amenti, A., Beyth, M, Dow, D.B., Temesgen, H., Hailu,
1064 T., 1978. Geological map of Adigrat area, Sheet ND 37-7. Ministry of Mines, Geological Survey
1065 of Ethiopia, Addis Ababa

1066 Kazmin, V., Seife, M.B., Nicoletti, M., Petrucciani, C., 1980. Evolution of the northern part of
1067 the Ethiopian Rift. Accad. Naz. Lincei, Rome 47, 275-291. NO DOI.

1068 Keir, D., Ebinger, C.J., Stuart, G.W., Daly, E., Ayele, A., 2006. Strain accommodation by
1069 magmatism and faulting as rifting proceeds to breakup: Seismicity of the northern Ethiopian rift.
1070 Journal of Geophysical Research 111, B05314. https://doi.org/10.1029/2005JB003748

1071 Keir, D., Hamling, I.J., Ayele, A., Calais, E., Ebinger, C., Wright, T.J., Jacques, E., Mohamed,
1072 K., Ham- mond, J.O.S., Belachew, M., Baker, E., Rowland, J.V., Lewi, E., Bennati, L. 2009.
1073 Evidence for focused magmatic accretion at segment centers from lateral dike injections captured
1074 beneath the Red Sea rift in Afar. Geology 37, 59-62. https://doi.org/10.1130/G25147A.1

1075 Kidane, T., 2015. Strong clockwise block rotation of the Ali-Sabieh/A¨isha Block: evidence for
1076 opening of the Afar Depression by a ‘saloon-door’ mechanism. From: Wright, T. J., Ayele, A.,
1077 Ferguson, D. J., Kidane, T. & Vye-Brown, C. (eds) Magmatic Rifting and Active Volcanism.
1078 Geological Society, London, Special Publications 420. http://doi.org/10.1144/SP420.10

Kirschner, J.P., Kominz, M.A., Mwakanyamale, K.E., 2010. Quantifying extension of passive margins: Implications for sea level change. Tectonics 29, TC4006. https://doi.org/10.1029/2009TC002557

Kogan, L., Fisseha, S., Bendick, R., Reilinger, R., McClusky, S., King, R., Solomon, T., 2012. Lithospheric strength and strain localization in continental extension from observations of the East African Rift. Journal of Geophysical Research 117, B03402. https://doi.org/10.1029/2011JB008516

La Rosa, A., Pagli, C., Keir, D., Sani, F., Corti, G., Wang, H., Possee, D., 2019. Observing oblique slip during rift linkage in northern Afar. Geophysical Research Letters, 46. https://doi.org/ 10.1029/2019GL084801

Le Gall B., Leleu S., Pik R., Jourdan F., Chazot G., Ayalew D., Yirgu G., Cloquet C., Chauvet F., 2018. The Red Beds series in the Erta Ale segment, North Afar. Evidence for a 6 Ma-old post-rift basin prior to continental rupturing. Tectonophysics 747–748, 373-389. https://doi.org/10.1016/j.tecto.2018.10.002

Leroy, S., d'Acremont, E., Tiberi, C., Basuyau, C., Autin, J., Lucazeau, F., Sloan, H., 2010. Recent off-axis volcanism in the eastern Gulf of Aden: Implications for plume–ridge interaction. Earth and Planetary Science Letters 293, 140–153. https://doi.org/10.1016/j.epsl.2010.02.036

Leroy, S., Razin, P., Autin, J., Bache, F., d'Acremont, E., Watremez, L. Robinet, J., Baurion, C., Denèle, Y., Bellahsen, N., Lucazeau, F., Rolandone, F., Rouzo, S., Serra-Kiel, J., Robin, C., Guillocheau, G., Tiberi, C., Basuyau, C., Beslier, M.-O., Ebinger, C., Stuart, G., Ahmed, A., Khanbari, K., Al Ganad, I., de Clarens, P., Patrick Unternehr, P., Khalfan Al Toubi, K., Lazki, Al., 2012. From rifting to oceanic spreading in the Gulf of Aden: a synthesis. Arabian Journal of Geosciences 5, 859-901. https://doi.org/10.1007/s12517-011-0475-4

Levell, B., Argent, J., Doré, G., Fraser, S., 2011. Passive margins: overview. From: Vining, B.A., Pickering, S.C. (eds) Petroleum Geology: From mature basins to new frontiers – Proceedings of the 7th Petroleum Geology Conference, 823–830. https://doi.org/10.1144/0070823

Makris, J., Ginzburg, A., 1987. The Afar Depression: transition between continental rifting and sea-floor spreading. Tectonophysics 141, 199–214. https://doi:10.1016/0040-1951(87)90186-7

Manighetti, I, Tapponnier, P., Courtillot, V., Gruszow, S., Gillot, P.-Y., 1997. Propagation of rifting along the Arabia-Somalia Plate Boundary: The Gulfs of Aden and Tadjoura. Journal of Geophysical Research 102, 2681-2710. https://doi.org/10.1029/96JB01185

Manighetti, I., Tapponnier, P., Gillot, P.Y., Jacques, E., Courtillot, V., Armijo, R., Ruegg, J.C., King, G., 1998. Propagation of rifting along the Arabia-Somalia plate boundary: Into Afar. Journal of Geophysical Research 103, 4947-4974. https://doi.org/10.1029/97JB02758

Manighetti, I., Taponnier, P., Courtillot, V., Gallet Y. Jacques, E., Gillot. P.-Y., 2001. Strain transfer between disconnected, propagating rifts in Afar. Journal of Geophysical Research 106, 13,613-13,665. https://doi.org/10.1029/2000JB900454

1116 Martin, A.K., 1984. Propagating rifts: Crustal extension during continental rifting. Tectonics 3,
1117 611-617. https://doi.org/10.1029/TC003i006p00611

1118 Medynski, S., Pik, R., Burnard, P., Dumont S., Grandin, R., Williams, A., Blarda, P.-H.,
1119 Schimmelpfennig, I., Vye-Brown, C., France, L., Ayalew, D., Benedetti, L., Yirgu, G., ASTER
1120 team, 2016. Magmatic cycles pace tectonic and morphological expression of rifting (Afar
1121 depression, Ethiopia). Earth and Planetary Science Letters 446, 77–88.
1122 http://dx.doi.org/10.1016/j.epsl.2016.04.014

1123 McClusky, S., Reilinger, R., Ogubazghi, G., Amleson, A, Healeb, B., Vernant, P., Sholan, J.,
1124 Fisseha, S., Asfaw, L., Bendick, R., Kogan, L., 2010. Kinematics of the southern Red Sea–Afar
1125 Triple Junction and implications for plate dynamics. Geophysical Research Letters 37, L05301.
1126 https://doi.org/10.1029/2009GL041127

1127 McKenzie, D.P., Davies, D., Molnar, P., 1970. Plate Tectonics of the Red Sea and East Africa.
1128 Nature 226, 243–248. https://doi.org/10.1038/226243a0

1129 Mohr, P., 1962. The Ethiopian rift system. Bulletin of the Geophysical Observatory, Addis
1130 Ababa 5, 33-62. NO DOI.

1131 Mohr, P., 1967. The Ethiopian Rift System. Bulletin of the Geophysical Observatory, Addis
1132 Ababa 11. 1-65. NO DOI.

1133 Mohr, P.A., 1972. Surface structure and plate tectonics of Afar. Tectonophysics 15, 3-9.
1134 https://doi.org/10.1016/0040-1951(72)90045-5

1135 Mohr, P., 1983a. Ethiopian flood basalt province. Nature 303, 577-584.
1136 https://doi.org/10.1038/303577a0

1137 Mohr, P., 1983b. The Morton-Black hypothesis for the thinning of continental crust – revisited in
1138 Western Afar. Tectonophysics, 94, 509-528. https://doi.org/10.1016/0040-1951(83)90032-X

1139 Mohr, P. & Zanettin, B., 1988. The Ethiopian flood basalt province. In: Macdougall, J. D. (ed.)
1140 Continental Flood Basalts. Dordrecht: Kluwer Academic, pp63-110.
1141 https://doi.org/10.1007/978-94-015-7805-9_3

1142 Molnar, N.E., Cruden, A.R., Betts, P.G., 2017. Interactions between propagating rotational rifts
1143 and linear rheological heterogeneities: Insights from three-dimensional laboratory experiments.
1144 Tectonics 36, 420-443. https://doi.org/10.1002/2016TC004447

1145 Molnar, N.E., Cruden, A.R., Betts, P.G., 2018. Unzipping continents and the birth of
1146 microcontinents. Geology 46, 451–454. https://doi.org/10.1130/G40021.1

1147 Mondy, L.S., Patrice, F.R., Duclaux, G., Mores, L., 2017. The role of asthenospheric flow during
1148 rift propagation and breakup. Geology 46, 103-106. https://doi.org/10.1130/G39674.1

1149 Morton, W.H., Black, R., 1975. Crustal attenuation in Afar. In: Pilger, A., Roster, A. (eds.) Afar
1150 Depression of Ethiopia, Schweizerbart, Stuttgart, 55-61. **NO DOI**

1151 Muirhead, J.D., Katterhorn, S.A., 2018. Activation of preexisting transverse structures in an
1152 evolving magmatic rift in East Africa. Journal of Structural Geology 106, 1-18.
1153 https://doi.org/10.1016/j.jsg.2017.11.004

1154 Muluneh, A.A., Kidane, T., Rowland, J., Bachtadse, V., 2013. Counterclockwise block rotation
1155 linked to southward propagation and overlap of sub-aerial Red Sea Rift segments, Afar
1156 Depression: Insight from paleomagnetism. Tectonophysics 593, 111–120.
1157 http://dx.doi.org/10.1016/j.tecto.2013.02.030

1158 Muluneh, A.A., Cuffaro, M., Doglioni, C., 2014. Left-lateral transtension along the Ethiopian
1159 Rift and constrains on the mantle-reference plate motions. Tectonophysics 632, 21-31.
1160 http://dx.doi.org/10.1016/j.tecto.2014.05.036

1161 Norcliffe, J.R., Paton, D.A., Mortimer, E.J., McCaig, A.M., Nicholls, H., Rodriguez, K.,
1162 Hodgson, N., Van der Spuy, D., 2018. Laterally Confined Volcanic Successions (LCVS);
1163 recording rift-jumps during the formation of magma-rich margins. Earth and Planetary Science
1164 Letters 504, 53-63. https://doi.org/10.1016/j.epsl.2018.09.033

1165 Pagli, C., Yun, S-H., Ebinger, C., Keir, D., Wang, H., 2019. Strike-slip tectonics during rift
1166 linkage. Geology 47, 31-34, doi: 10.1130/G45345.1.

1167 Paton, D.A., Pindell, J., McDermott, K., Bellingham, P., Horn, B., 2017. Evolution of seaward-
1168 dipping reflectors at the onset of oceanic crust formation at volcanic passive margins: Insights
1169 from the South Atlantic. Geology 45, 439-442. https://doi.org/10.1130/G38706.1

1170 Purcell, P.G., 2017. Re-imagining and re-imaging the development of the East African Rift.
1171 Petroleum Geoscience, 24, 21-40. https://doi.org/10.1144/petgeo2017-036

1172 Redfield, T.F., Wheeler, W.H., Often, M., 2003. A kinematic model for the development of the
1173 Afar Depression and its paleogeographic implications. Earth and Planetary Science Letters, 216,
1174 383-398. https://doi.org/10.1016/S0012-821X(03)00488-6

1175 Reilinger, R., McClusky, S., 2011. Nubia–Arabia–Eurasia plate motions and the dynamics of
1176 Mediterranean and Middle East tectonics. Geophysical Journal International. 186, 971-979.
1177 https://doi.org/10.1111/j.1365-246X.2011.05133.x

1178 Roberts, G.P., Michetti. A.M., 2004. Spatial and temporal variations in growth rates along active
1179 normal fault systems: an example from The Lazio–Abruzzo Apennines, central Italy. Journal of
1180 Structural Geology 26, 339–376. https://doi.org/10.1016/j.jsg.2017.11.004

1181 Rooney, T.O., 2017. The Cenozoic magmatism of East-Africa: Part I — Flood basalts and pulsed
1182 magmatism. Lithos 286-287, 264-301. https://doi.org/10.1016/j.lithos.2017.05.014

1183 QGIS Development Team, 2009. QGIS Geographic Information System. Open Source
1184 Geospatial Foundation. http://qgis.osgeo.org

1185 Sani, F., Ghinassi, M., Papini, M., Oms, O., Finotello, A., 2017. Evolution of the northern tip of
1186 Afar triangle: inferences from the Quaternary succession of the Dandiero – Massawa area
1187 (Eritrea). Tectonophysics 717, 339-357. https://doi.org/10.1016/j.tecto.2017.08.026

1188 Saria, E., Calais, E., Stamps, D.S., Delvaux, D., Hartnady, C.J.H., 2014. Present-day kinematics
1189 of the East African Rift. Journal of Geophysical Research: Solid Earth, 119, 3584-3600.
1190 https://doi.org/10.1002/2013JB010901

1191 Sichler, B., 1980. La biellette Danakile; un modele pour l'evolution geodynamique de l'Afar.
1192 Bulletin de la Société Géologique de France, S7-XXII, 925-932.
1193 https://doi.org/10.2113/gssgfbull.S7-XXII.6.925

1194 Smith, J.V., 1993. Infinitesimal kinematics of rotational rifting with reference to en echelon
1195 marginal faults in the Red Sea region. Tectonophysics 222, 227-235.
1196 https://doi.org/10.1016/0040-1951(93)90050-T

1197 Souriot, T., Brun, J.-P., 1992. Faulting and block rotation in the Afar triangle, East Africa: The
1198 Danakil “crank-arm” model. Geology 20, 911-914. https://doi.org/10.1130/0091-
1199 7613(1992)020<0911:FABRIT>2.3.CO;2

1200 Stab, M., Bellahsen, N., Quicelleur, X., Ayalew, D., Leroy, S., 2016. Modes of rifting in magma-
1201 rich settings: Tectonomagmatic evolution of Central Afar. Tectonics, 35, 2-38.
1202 https://doi.org/10.1002/2015TC003893

1203 Straume, E.O., Gaina, C., Medvedev, S., Hochmuth, K., Gohl, K., Whittaker, J. M., Abdul
1204 Fattah, R., Doornenbal. J.C., Hopper, J.R., 2019. GlobSed: Updated total sediment thickness in
1205 the world's oceans. Geochemistry, Geophysics, Geosystems, 20.
1206 https://doi.org/10.1029/2018GC008115

1207 Szymanski, E., Stockli, D.F., Johnson, P.R., Hager, C., 2016. Thermochronometric evidence for
1208 diffuse extension and two-phase rifting within the Central Arabian Margin of the Red Sea Rift.
1209 Tectonics 35, 2863–2895. https://doi.org/10.1002/2016TC004336

1210 Tadesse, N., Nedaw, D., Woldearegay, K., Gebreyohannes, T., Van Steenbergen, F., 2015.
1211 Groundwater management for irrigation in the Raya and Kobo Valleys, Northern Ethiopia.
1212 International Journal of Earth Sciences and Engineering, 8, 36-46.
1213 http://cafetinnova.org/innova/archiveList/IJEE/2015/03/02080305.pdf

1214 Tesfaye, S., Harding, D.J., Kusky, T.M., 2003. Early continental breakup boundary and
1215 migration of the Afar triple junction, Ethiopia. GSA Bulletin 115, 1053-1067.
1216 https://doi.org/10.1130/B25149.1

1217 Tesfaye, S., Ghebreab, W., 2013. Simple shear detachment fault system and marginal grabens in
1218 the southernmost Red Sea rift. Tectonophysics 608, 1268–1279.
1219 http://dx.doi.org/10.1016/j.tecto.2013.06.014

1220 Tugend, J., Gillard, M., Manatschal, G., Nirrengarten. M., Harkin, C., Epin, M.-E., SAuter, D.,
1221 Autin, J., Kusznir, N., McDermott, K., 2018. Reappraisal of the magma-rich versus magma-poor

rifted margin archetypes. In: McClay, K.R., Hammerstein, J.A. (eds) Passive Margins: Tectonics, Sedimentation and Magmatism. Geological Society, London, Special Publications 476. https://doi.org/10.1144/SP476.9

Van der Pluijm, B.A., Marshak, S., 2004. Earth Structure, 2nd edition. W.W. Norton & Company Ltd., New York.

Varet, J., 2018. Geology of Afar. Springer International Publishing AG.

Vink, G.E., 1982. Continental rifting and the implications for plate tectonic reconstructions. Journal of Geophysical Research 87, 10,667-10,688. https://doi.org/10.1029/JB087iB13p10677

Wessel, P., Luis, J.F., 2017, The GMT/MATLAB Toolbox, Geochem. Geophys. Geosyst., 18, 811-823. http://dx.doi.org/10.1002/2016GC006723

Williams, F.M., 2016. Understanding Ethiopia. Springer International Publishing https://doi.org/10.1007/978-3-319-02180-5

Wolfenden, E., Ebinger, C., Yirgu, G., Deino, A., Ayalew, D., 2004. Evolution of the northern Main Ethiopian rift: birth of a triple junction. Earth and Planetary Science Letters 224, 213-228. https://doi.org/10.1016/j.epsl.2004.04.022

Wolfenden, E., Ebinger, C., Yirgu, G., Renne, P.R., Kelley, S.P., 2005. Evolution of a volcanic rifted margin: Southern Red Sea, Ethiopia. GSA Bulletin 117, 846-864. https://doi.org/10.1130/B25516.1

Wright, T. J., Ebinger, C., Biggs, J., Ayele, A., Yirgu, G., Keir, D., & Stork, A., 2006. Magma-maintained rift segmentation at continental rupture in the 2005 Afar dyking episode. Nature 442 (7100), 291-294. DOI: 10.1038/nature04978

Zanettin, B., Justin-Visentin, E. 1975. Tectonical and volcanological evolution of the western Afar margin (Ethiopia). In: Pilger, A., Roster, A. (eds.) Afar Depression of Ethiopia, Schweizerbart, Stuttgart, 300-309. No DOI

Zou, C., Zhai, G., Zhang, G., Wang, H., Zhang, G., Li, J., Wang, Z., Wen, Z., Ma, F., Lang, Y., Li, X., Liang, K., 2015. Formation, distribution, potential and prediction of global conventional and unconventional hydrocarbon resources. Petroleum Exploration and Development 42, 14-28. https://doi.org/10.1016/S1876-3804(15)60002-7

Zwaan, F., Corti, G., Keir, D., Sani, F., 2020a. A review of tectonic models for the rifted margin of Afar: implications for continental break-up and passive margin formation. Journal of African Earth Sciences. https://doi.org/10.1016/j.jafrearsci.2019.103649

Zwaan, F., Schreurs, G., Rosenau, M. 2020b. Rift propagation in rotational versus orthogonal extension: insights from 4D analogue models. Journal of Structural Geology, 103946. https://doi.org/10.1016/j.jsg.2019.103946

Zwaan, F., Corti, G., Keir, D., Sani, F., Muluneh, A., Illsley-Kemp, F., Papini, M., 2020c. Geological data from the Western Afar Margin, East Africa. GFZ Data Services. http://doi.org/10.5880/fidgeo.2020.017